Title
ELECTROCHEMICAL STORAGE CELL BASED ON POLYCRYSTALLINE SILICON

Authors
Canfield, D.
Morrison, S.R.

Publication Date
1982-02-01

LBL-14639
UC-94cb c.2

Lawrence Berkeley Laboratory
UNIVERSITY OF CALIFORNIA

ENERGY & ENVIRONMENT DIVISION

ELECTROCHEMICAL STORAGE CELL BASED ON POLYCRYSTALLINE SILICON

Duane Canfield and S. Roy Morrison

February 1982

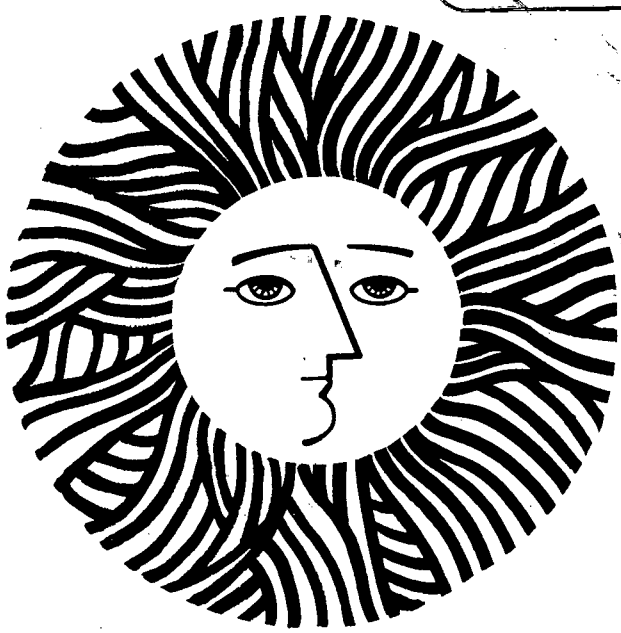

Prepared for the U.S. Department of Energy under Contract DE-AC03-76SF00098

DISCLAIMER

February 28, 1982

Final Report
Covering the Period from
1 March 1981 to 1 March 1982

ELECTROCHEMICAL STORAGE CELL BASED ON POLYCRYSTALLINE SILICON

By: Duane Canfield and S. Roy Morrison

Prepared for:

LAWRENCE BERKELEY LABORATORY
University of California
#1 Cyclotron Road
Berkeley, California 94720

Attention: Dr. Frank McLarnon

Subcontract No. 4510610
SRI International Project No. PYU 2857

Approved:

D. L. Hildenbrand

D. L. Hildenbrand, Director
Materials Research Laboratory

G. R. Abrahamson
Vice President
Physical Sciences Division

PROJECT SUMMARY

During this year of the program on the photoelectrochemical storage cell, we conducted theoretical and experimental investigations on the performance of n- and p-type silicon in solution for efficient solar energy conversion.

In our experimental work we sought to identify redox couples capable of inducing maximum band bending (highest open circuit voltage) and limit the corrosion for both n- and p-type silicon. Measurements showed that high photovoltages could be obtained by using vanadium (II/III) and ferrocene/ferricenium couples for p-type and n-type silicon, respectively. With these systems we demonstrated reasonable stability even though these couples were incapable of producing a high efficiency. The low efficiencies were caused by the growth of a relatively thick insulating SiO_2 corrosion layer. Under conditions of low light intensity, however, a thin ($\sim$ 15 Å) SiO_2 layer enhanced the solar cell characteristics.

We performed corrosion studies to evaluate the use of HF to remove the corrosion layer. In these experiments we also had to consider the interaction between HF and the redox couple. We found that high or low concentrations of HF accelerate the corrosion of the surface. Redox couples may play different roles in this corrosion. Some redox couples are not affected by the HF and do not suppress corrosion, while others catalyze the corrosion of the semiconductor by HF.

Much of the experimental and theoretical work focused on the effect of the surface oxide on solar cell characteristics. These studies in turn led to a variety of surface treatments aimed at improving the fill factor of silicon photoelectrochemical cells. The surface treatments included high temperature annealing of the normal oxide under an argon or hydrogen atmosphere, coating a p-n junction with a thin layer of platinum, and passivation with poly-vinylcarbazole polymer.

The major conclusions from our study are outlined below. The silicon electrode is subject to severe corrosion problems. This corrosion leads to highly insulating thin films of SiO_2 which block the photocurrent. Thus, the silicon electrode must be completely stabilized to realize high efficiency and acceptable cell life. Our studies indicate the required stability will probably not be achieved on a bare Si surface.

Up to now the most promising method for stablizing the Si is by application of thin metal films. However, the use of conducting surface films leads to a loss of open circuit voltage because of enhanced dark currents. Thick layers of conducting material also block the incoming light. Further studies using less active conducting polymer films might lead to new stable systems. At the present time, it appears that enhanced stability may be achieved only with a loss of efficiency.

Other semiconductor materials such as CdSe may be more promising. High photovoltages ($\sim$ 1.0 V) and conversion efficiencies

(~ 12% single crystal) have been obtained. However, corrosion problems with this electrode have not been completely solved. It is clear that corrosion is the most important bottleneck to the development of devices utilizing the photoelectrochemical approach.

Publications:

The Effect of Surface Films on Photoelectrochemical Solar Cell Performance, D. Canfield and S. R. Morrison, Appl. Surf. Sci., in press.

Surface Films on Semiconductor, S. R. Morrison, ACS Meeting, Las Vegas.

CONTENTS

ILLUSTRATIONS

I INTRODUCTION

A. Objective

The objective of this study was to develop a practical photoelectrochemical storage solar cell based on silicon, a material that has a favorable bandgap, and is available at low cost.

Proposed was a new solar battery configuration based on the storage system, $Sb^{5+}/Sb^{3+}/Sb$. This system is adaptable to silicon cells both because of the voltage requirements and because silicon is resistant to corrosion by the antimony chlorides. The main potential problem was the formation of oxide on the silicon surface. Thus the emphasis of research was directed toward practical control of the formation of such oxide layers. A second major goal was to determine, from many possible redox couples, a suitable redox couple to induce the maximum photovoltage from silicon. These two goals, the selection of a system to resist the formation of insulating layers of silicon oxide and the selection of a system to optimize the open circuit voltage of silicon, were the focus of the program. All narrow bandgap semiconductors studied to date have shown corrosion problems that must be considered the dominant difficulty in developing a good photoelectrochemical cell for either photovoltaic or storage purposes.

B. Choice of Materials

The design of the photobattery under study is shown in Fig. 1. The device should be able to store energy under illumination and give energy when a load is placed over its terminals (T). We are investigating p- and n-type silicon for the photoactive material. Silicon has a suitable bandgap, a very well-established technology, and a low manufacturing cost when the demands for purity levels and crystallinity are not too high. If the photobattery uses the liquid-junction approach (silicon in direct contact with the redox electrolyte), the requirements for the silicon become much less stringent than those for a solid/solid junction that has either p- and n-type silicon or silicon and metal. Indeed, the barrier formed at the solid-liquid interface has been proved[1]

to be much less sensitive toward all kinds of defects on the silicon than the more classical barriers formed with a p-n junction or a metal/semiconductor Schottky barrier. Therefore, we would aim for using a low-cost polycrystalline sheet of silicon. However, we used single crystal silicon in this study.

C. Cell Operation

Briefly, the cell's operation as a combined photocell and storage battery is as follows: The p- and n-type silicon photoelectrochemical (PEC) cells, shown in the top half of Fig. 1, develop a photovoltage. This photovoltage appears across the $Sb/Sb^{3+}/Sb^{5+}$ cell, shown in the lower half of Fig. 1. During charging, the photovoltage in the silicon drives positive current from the n-silicon into the positive redox couple solution, and then through the metal to the negative redox couple solution, and into the p-silicon. On the "battery" side of the cell, this positive current coming from the p-silicon oxidizes the Sb^{+3} to Sb^{+5}, passes through the separator, and, while reducing Sb^{+3} to Sb, completes the circuit at the n-silicon electrode. Thus, the photocurrent charges the antimony cell. The antimony cell can be discharged at any time, drawing power from the top "T" electrodes.

This design load-levels the solar input. A minor increase in cell volume over the PEC cell alone permits storage of solar energy.

As discussed in previous reports, we can reach a photovoltage of greater than 1 V with the combined n- and p-silicon photocells. Thus, a storage system based on $Sb/Sb^{3+}/Sb^{5+}$ (open circuit voltages, OCV = 0.8-0.9 V) as indicated in Fig. 1 may be feasible.

An advantage of redox batteries with the antimony storage system is that problems with the separator are minimized. Because the same ion is used for each couple in the redox systems, the system is much less sensitive to interdiffusion between cells. Thus, a relatively low-cost separator can be used. This substantially reduces the cost of the battery, which is a dominant concern in solar conversion systems.

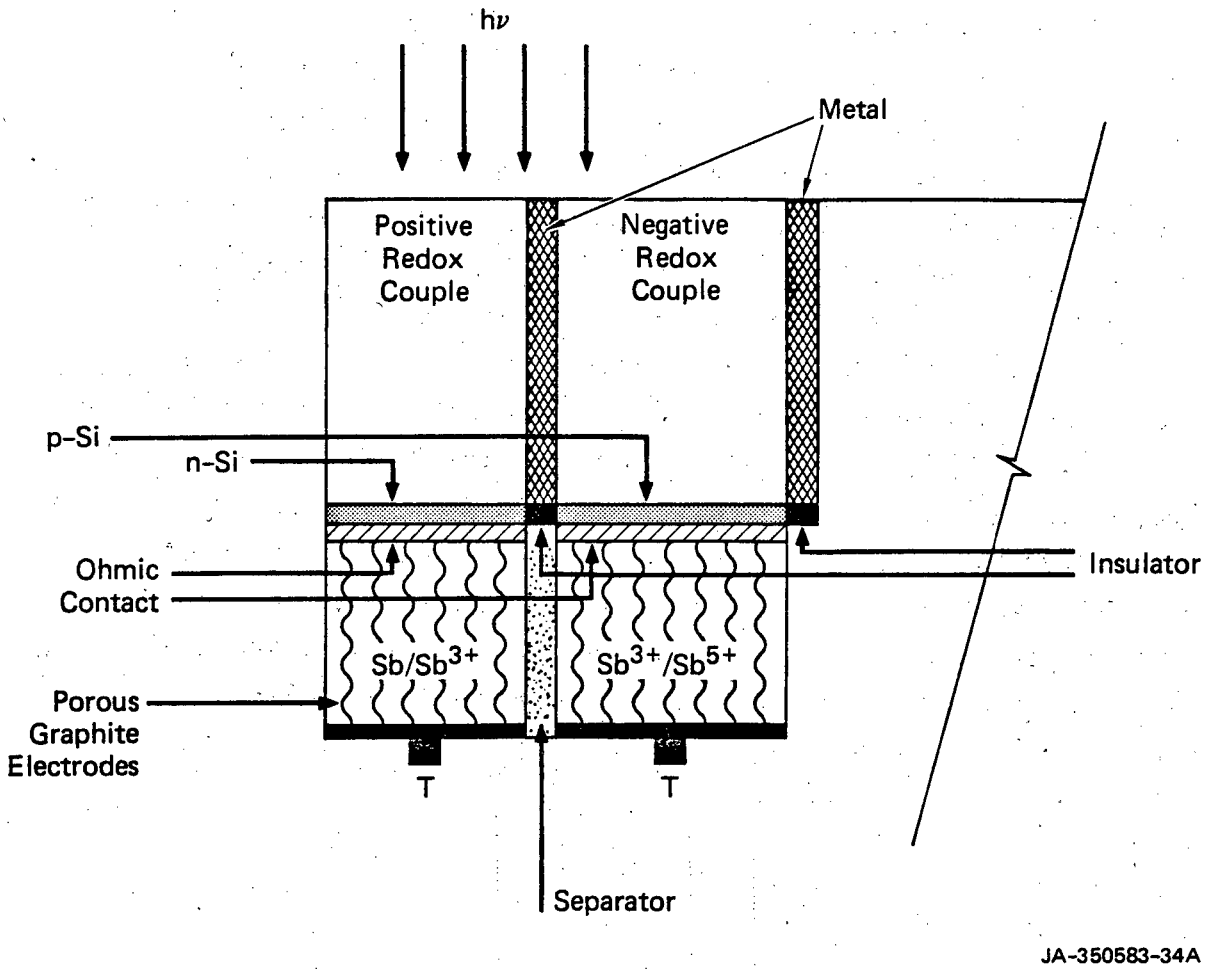

FIGURE 1 SUGGESTED DESIGN FOR PHOTOBATTERY

D. Research Plan

The primary issue in the first year was choosing a suitable redox couple(s) for the top compartment(s) to give a high photovoltage and low corrosion.

To obtain maximum photovoltage, we needed a redox couple with an energy level E°_{redox} near the edge of the minority carrier band. In earlier studies[2] we have determined the flat band potentials of n- and p-type silicon as given in Figs. 2 and 3, respectively. Thus, for n-silicon, with a conduction band edge of -4.0 eV vs. vacuum, the desired redox couple has an E^{o} near +0.2 V SCE at pH 7.0 and for p-silicon, the desired redox couple has an E^{o} near -0.9 V SCE. Figure 4 shows the reason for the choice: the high band bending expected on n-silicon with N,N,N',N'-tetramethyl-p-phenylenediamine (TMPD) present leads to a high OCV. That voltage is not as high as Fig. 4 indicates - photo-produced holes collect at the surface, giving rise to a voltage, until the surface barrier is low enough for electrons to move to the surface recombination centers at the same rate as holes. Thus, for maximum OCV, the redox couple must have a favorable redox potential; at the same time, it must not effectively promote recombination.

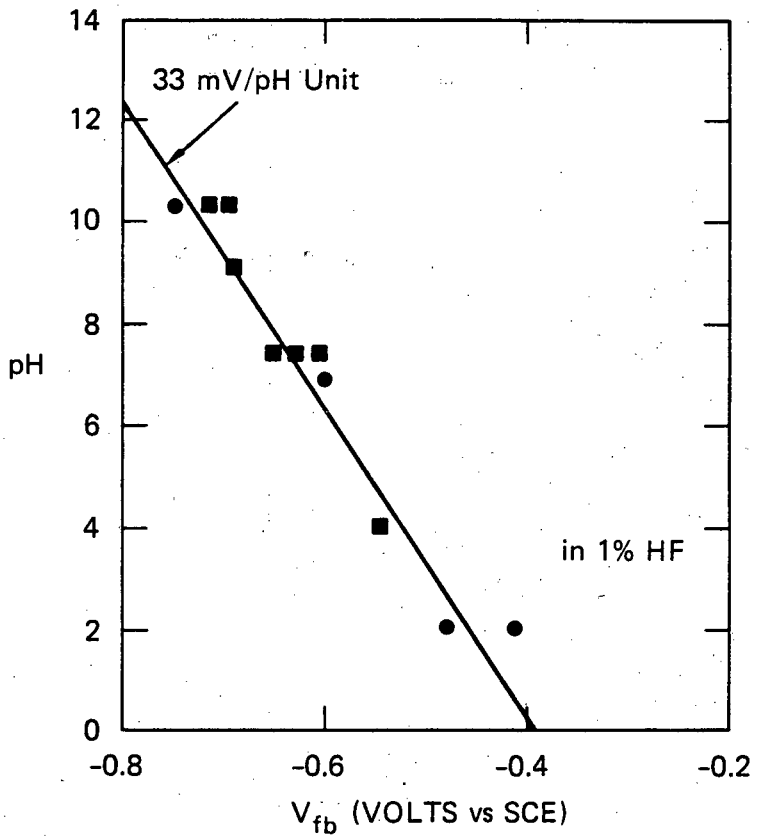

FIGURE 2 FLATBAND POTENTIAL V_{fb} VERSUS pH FOR n-SILICON IN 0.1 M $K_4Fe(CN)_6$ AQUEOUS SOLUTION

● and ■ describe adjustments in pH by the addition of HCl on NH_4OH.

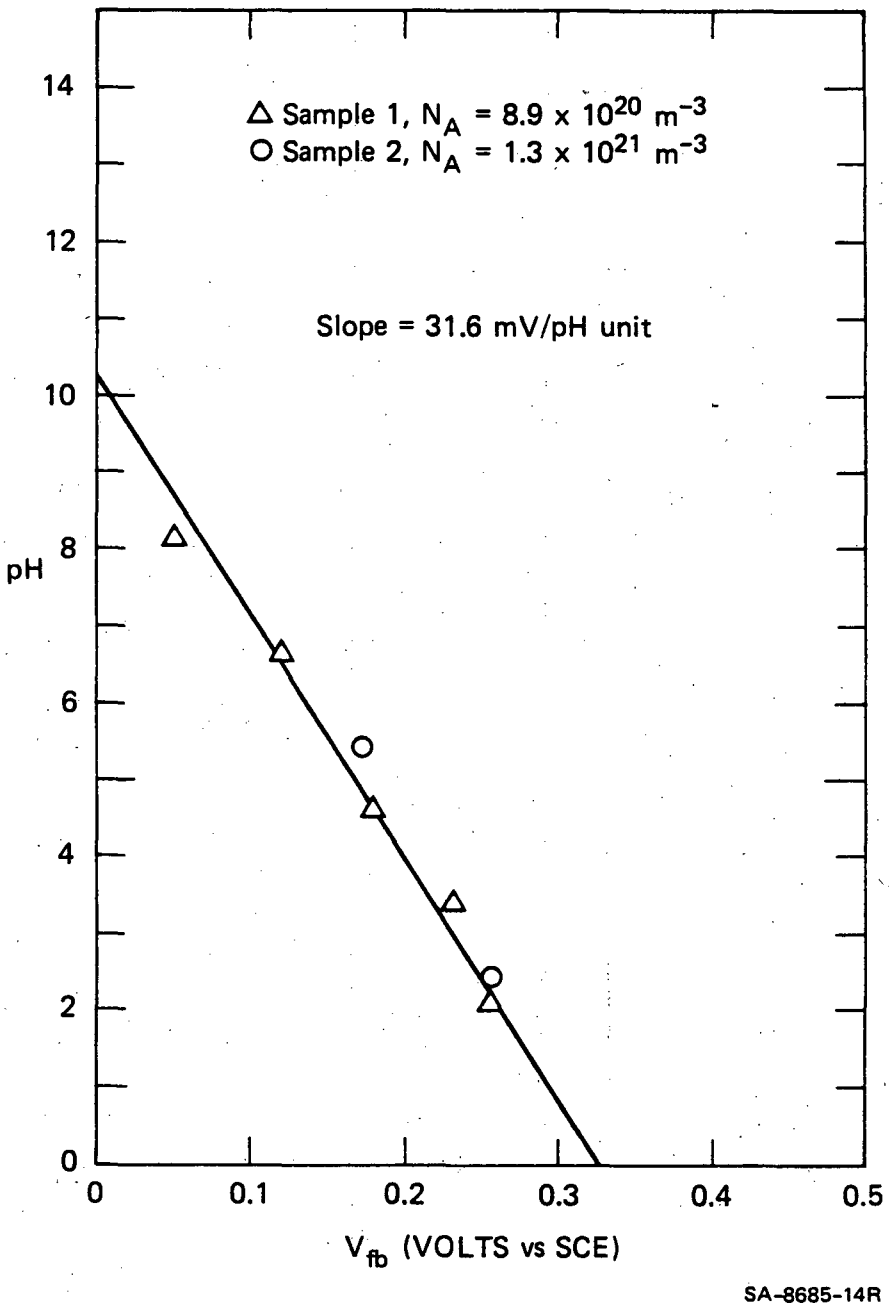

FIGURE 3 FLATBAND POTENTIAL V_{fb} VERSUS pH FOR p-SILICON IN THE PRESENCE OF Fe(II)EDTA

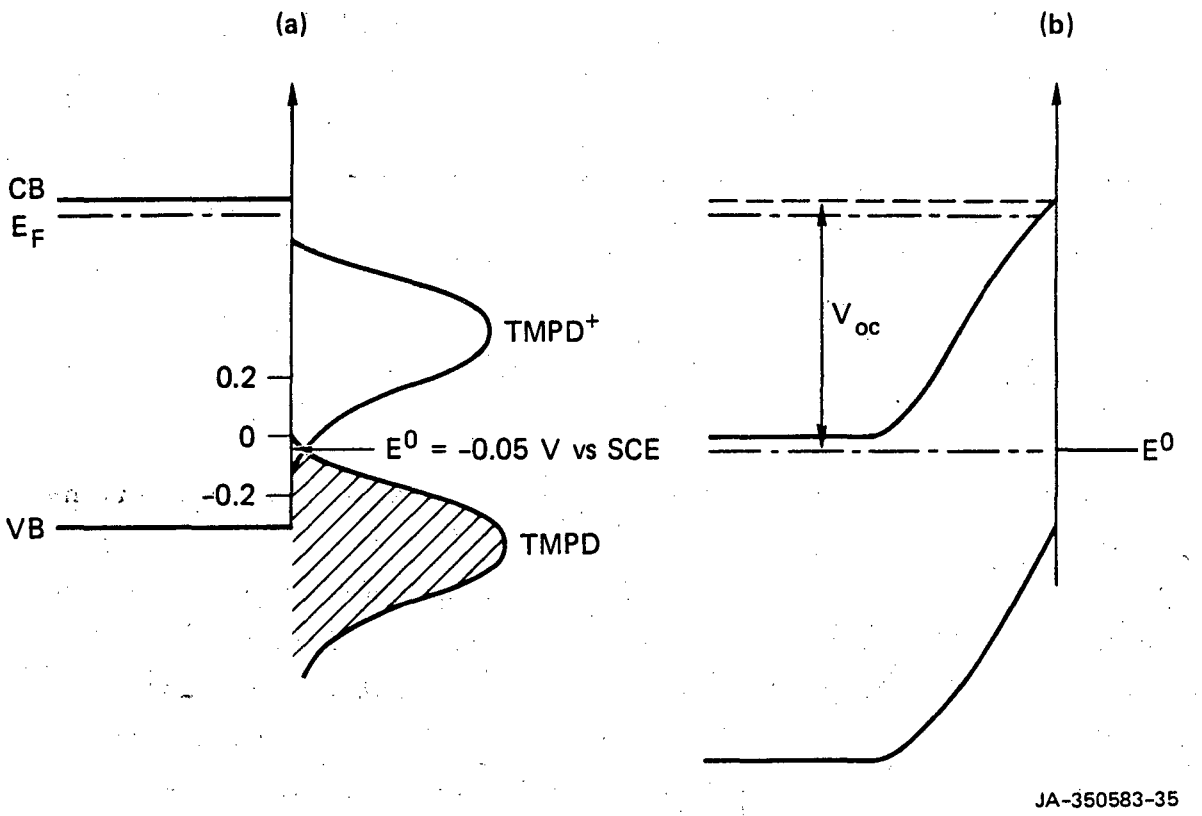

FIGURE 4 INTERFACIAL ENERGETICS FOR n-SILICON

Absolute energy levels (a);
Semiconductor-solution contact (b).

II REDOX COUPLES AND CORROSION

The studies on n- and p-type silicon will be discussed separately because the problems and approaches differ. Note that the problems with p-type silicon were solved much more easily than originally anticipated and that the problems with n-silicon were much more difficult to solve.

A. n-Type Silicon

The investigation of n-type silicon has been directed toward solving three interrelated problems:

1. Development of a high photovoltage, OCV.
2. Development of a high current density, I_{scc}
3. Minimization of oxide growth.

The formation of an insulating layer of oxide results in electron-hole recombination by a surface state, and in an additional resistance in the circuit. With these effects, the oxide has a dominating role in determining both photovoltage and photocurrent. As discussed in the introduction, the driving force for a cell, the photovoltage, is determined not only by the relative energy levels of the valence and conduction bands of the semiconductor to the potential of the redox couple, but also, in part, by surface state recombination. The current density I_{scc} (short circuit) is affected by recombination, as well as by the added series resistance.

In order to drive the antimony energy storage system (Fig. 1), 0.9 V will have to be produced from the combination of n- and p-type silicon. The sum of the OCVs, the maximum voltage attainable, must exceed this amount, to allow for the passage of current. Ideally, the sum should exceed 0.9 V to permit operation of the solar cell at maximum efficiency.

The oxide problem is particularly important on n-type semiconductors because they are subject to surface oxidation by combining with water. This problem is accentuated by water, which may react with accumulated holes at the silicon surface.

Initial experiments in aqueous solutions of iron cyano and iron ethylenediamine tetraacetic acid EDTA couples have demonstrated that after a short time, the formation of an oxide greatly reduces the current, as shown in Figure 5. When an etchant is added to the solution to remove the oxide, the current density of the electrode remains stable for a short period at a lower value, then eventually decreases to zero. More will be said about the corrosion in solutions containing HF. The major problem with the iron (cyano) or iron (EDTA) couples is that the photovoltages are low, about 0.2 to 0.4 volts respectively. Low photovoltages for n-silicon in water seem to be the rule, because of the difficulty in finding an aqueous redox couple capable of inducing maximum band bending.

We have also investigated nonaqueous solvents. Although oxide formation may continue in a nonaqueous solvent because of small amounts of dissolved water or solvent breakdown, the rate at which an oxide grows is markedly decreased. The most favorable redox couples in nonaqueous solutions for n-type silicon have been TMPD and ferrocene.

The maximum observed OCV of n-type silicon in TMPD/$TMPD^+$ dissolved in methanol has been 0.54 V. This can be obtained when the surface of the electrode is free from an insulating amount of oxide (<20 Å). The oxide is normally about 15-20 Å thick after cleaning with HF. Such an OCV, 0.54 V is greater than half the voltage needed to store energy using the system shown in Fig. 1.

Figure 6 illustrates typical current-voltage characteristics of n-type silicon in TMPD/methanol; it is clear that the system needs some improvement. First, the OCV is somewhat lower than the 0.54 V reported above, because of an insulating layer of silicon oxide. Second, the fill factor of the power curve is low (ff = 0.12). The current density in the device is also limited, presumably because of recombination and a resistive oxide.

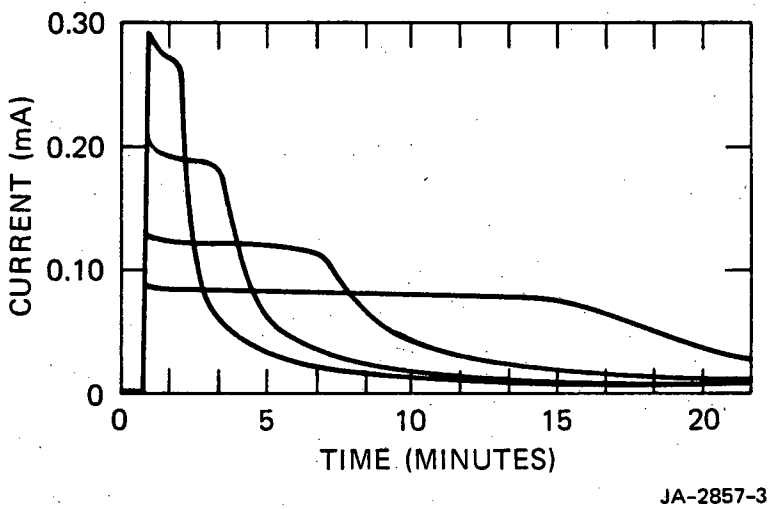

FIGURE 5 n-TYPE Si STABILIZATION TIME IN 0.1 M $F_e(CN)_6^{4-}$ AT +1.0 VOLTS VS. SCE

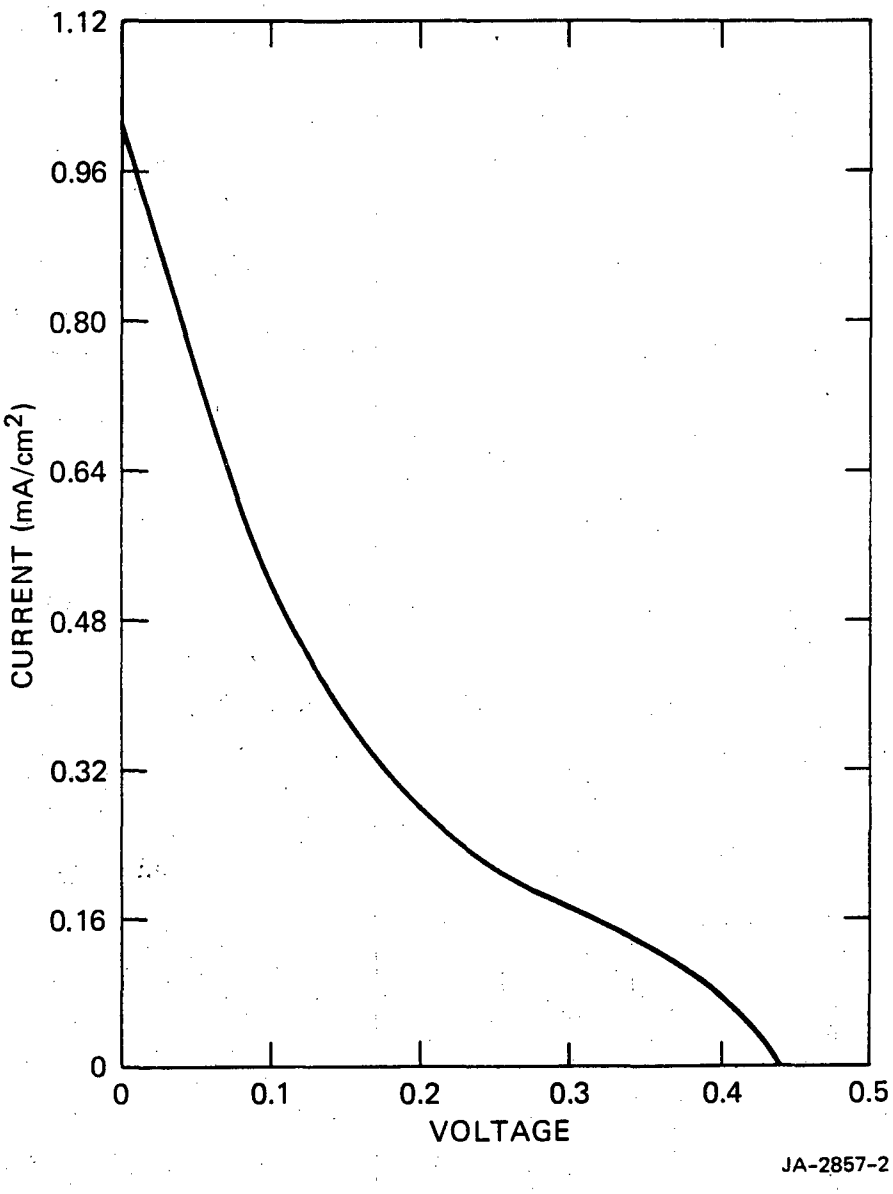

FIGURE 6 POWER CURVE FOR n-Si IN TMPD/MeOH

Unfortunately, with this system, the addition of HF to remove the oxide leads to other complications. Specifically, rather than improving, the current-voltage characteristics of n-type silicon become less favorable.

Greater OCV can be obtained by using the non-aqueous ferrocene/ferricenium couple in absolute ethanol.[2] On n-type silicon, a voltage of 0.62 V can be obtained. However, there are limitations on the current with this system. The charge transfer process at the electrode-electrolyte interface is slow. We found that the current density in the ferrocene/ferricenium system (saturated solution) is 0.83 mA/cm^2 (SCC).

B. p-Type Silicon

The decomposition problems on p-type semiconductors in solution are not so serious as those on n-type semiconductors. At ordinary voltages these electrodes do not accumulate holes which weaken the lattice of the crystal. Therefore p-type silicon can be used in aqueous solution with less stringent requirements on electron transfer rates.

According to our studies, the vanadium and chromium redox couples are best suited for inducing maximum band bending in p-type silicon, which results in a large photovoltage. Figure 7 illustrates the power curve for a p-type electrode in an acidic solution of 0.07 M V^{+2}/0.07 M V^{+3}. No HF is present. A photovoltage of 0.51 and short circuit of about 5 mA can be obtained. As with n-type, p-type silicon exhibits low fill factors (ff = 0.17), because of the abundance of surface states caused by the thin layer of silicon dioxide already present on the electrode surface. If oxygen is excluded from the cell, vanadium II remains stable in solution, and the negative potential is maintained. In such an oxygen-free solution, the cell was tested at 1.5 mA/cm^2 at 0.28 volts for 48 hours, and there was no significant decrease in power.

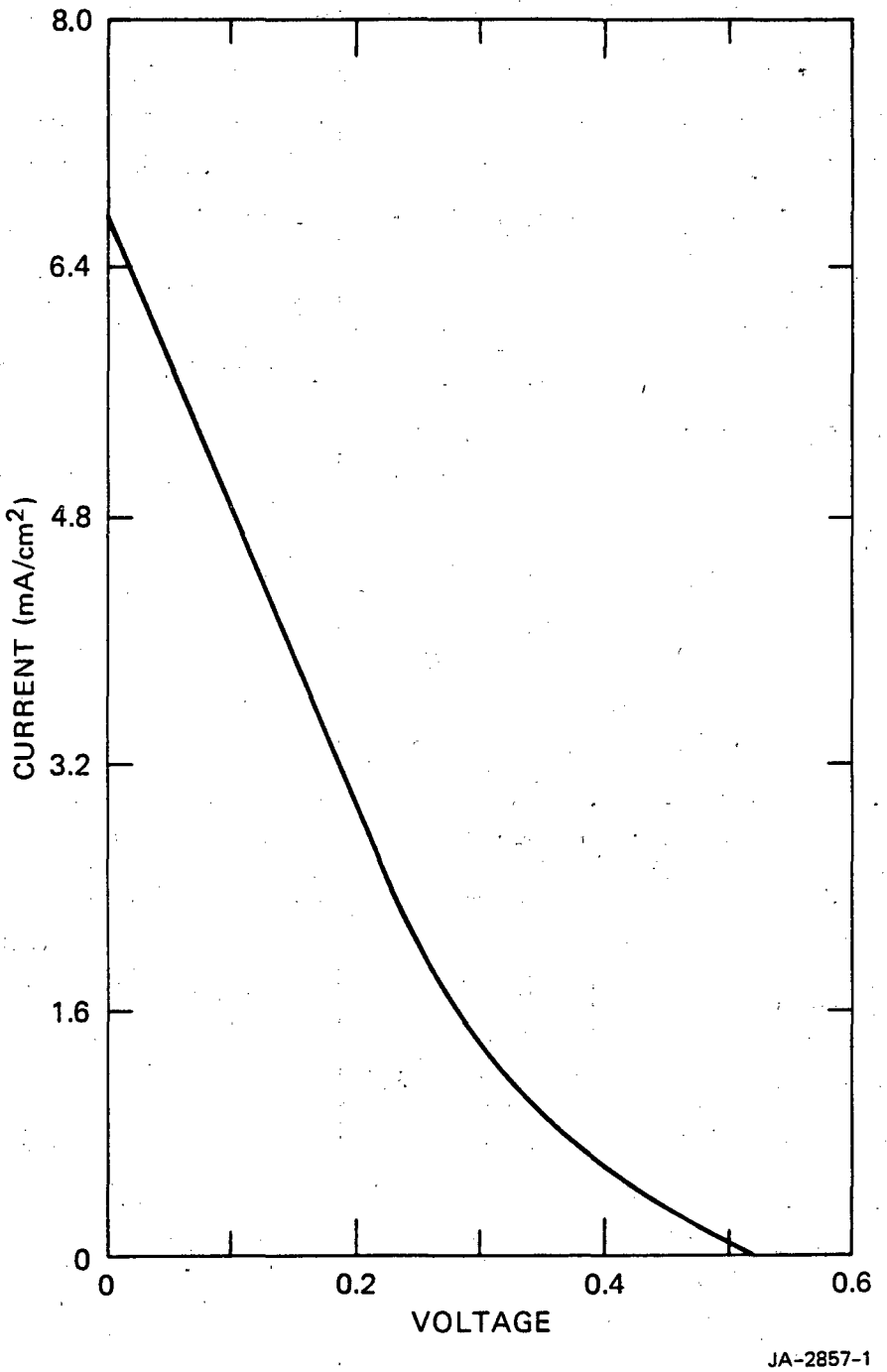

FIGURE 7 POWER CURVE FOR p-Si IN VANADIUM II/III

A greater OCV, V = 0.62, can be obtained using the chromium (II/III) couple, which has a more negative formal redox potential than the vanadium couple (-0.41 and -0.255 vs NHE, respectively). However stabilizing chromium II is more difficult, because it is more easily oxidized. Another problem with the chromium couple is that, in very acidic solutions, hydrogen is evolved from the surface of illuminated silicon, decreasing the efficiency of the cell and making the solution unstable.

Table 1 summarizes the best results for the chromium couple, the vanadium couple, and other couples tested. The results follow well the expected relation (see Introduction) between the OCV and the redox potential of the couple.

Table 1

ELECTROCHEMICAL POTENTIALS OF VARIOUS REDOX COUPLES

Redox Couple	E^o (SCE)	Electrolyte Potential (SCE)	Maximum Photovoltage (V_{oc})
$Cr^{3/2}$	-0.98	-0.60	-0.62
$V^{3/2}$	-0.497	-0.46	-0.51
Fe (citrate) pH 8.2	-0.45	-0.318	-0.244
Fe (EDTA) pH 8.8	-0.12	-0.240	-0.240
$Sn^{4/2}$ pH 1.6	0.15	-0.05	-0.40

C. Surface Corrosion

For the successful operation of the energy storage system, the thickness of the oxide layer on silicon photoelectrodes must be minimized. We have conducted experiments to relate the oxide dissolution rate to the composition of the solution.

Redox couples by themselves cannot stabilize a photoelectrode. Depending upon the stabilization efficiency of the system (electrode, redox couple, solution), a relative fraction of photoproduced holes will corrode the electrode surface. For this reason, either the solution or something added to the solution must minimize the corrosion effect. In the silicon photoelectrochemical system, if the redox couple (stabilizing agent) absorbs holes with an efficiency greater than 99%, then, with the addition of HF to the solution, perhaps the oxide thickness could be minimized, allowing efficient operation of the cell.

Figure 8 illustrates the dissolution rate of a thin anodic oxide from photocorroding silicon. The photocurrent is monitored as a function of light intensity, with no stabilizing agent present. When the rate of oxide removal by the etchant becomes lower than the rate of oxide formation by photoproduced holes, the current density becomes nonlinear with light intensity. The results (Fig. 8) indicate that 0.05 M HF can remove oxide at a rate up to 0.06 mA/cm^2. However, in the presence of a stabilizing agent (ferrocyanide ion), HF promotes the initial stages of oxide growth. In these experiments, n-type silicon was washed with HF before being exposed to a solution containing 0.20 M $K_4Fe(CN)_6$ and varying concentrations of NH_4F. The acidity was adjusted by additions of HCl. Therefore, the concentration of HF will be determined by the limiting factor of NH_4F concentration or pH.

HF promotes oxide growth by strongly interacting with silicon at the Si/SiO_x interface. Figures 9 and 10 illustrate the effect of low concentrations of HF (a sharp drop in photocurrent), compared with no HF (normal photocurrent decay). In Fig. 10, curves a and b, the

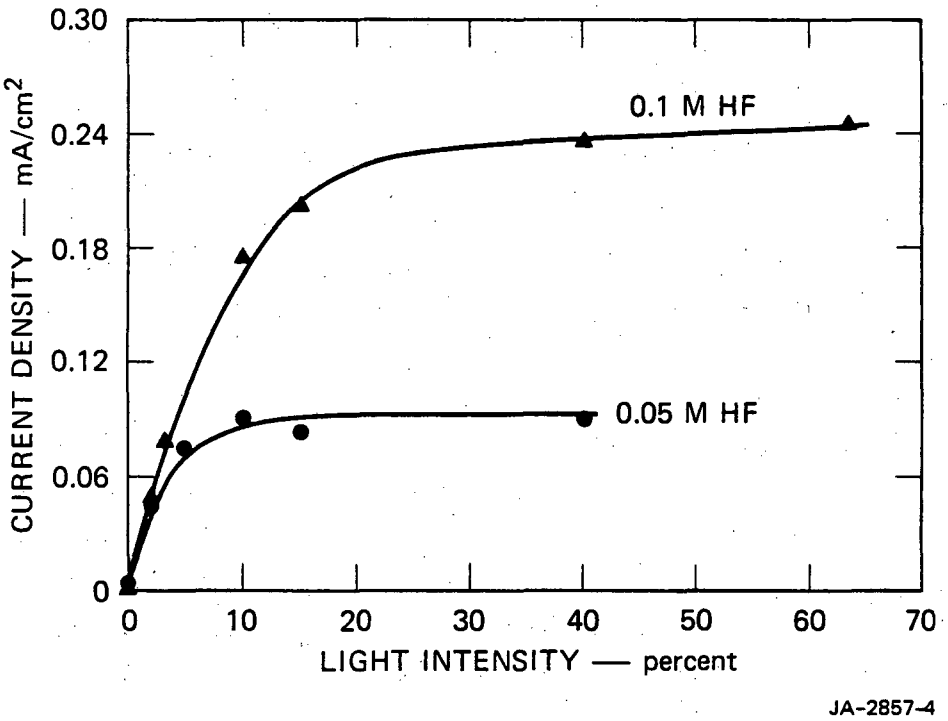

FIGURE 8 LIMITING CURRENT AS A FUNCTION OF LIGHT INTENSITY RELATIVE TO CONCENTRATION OF HF

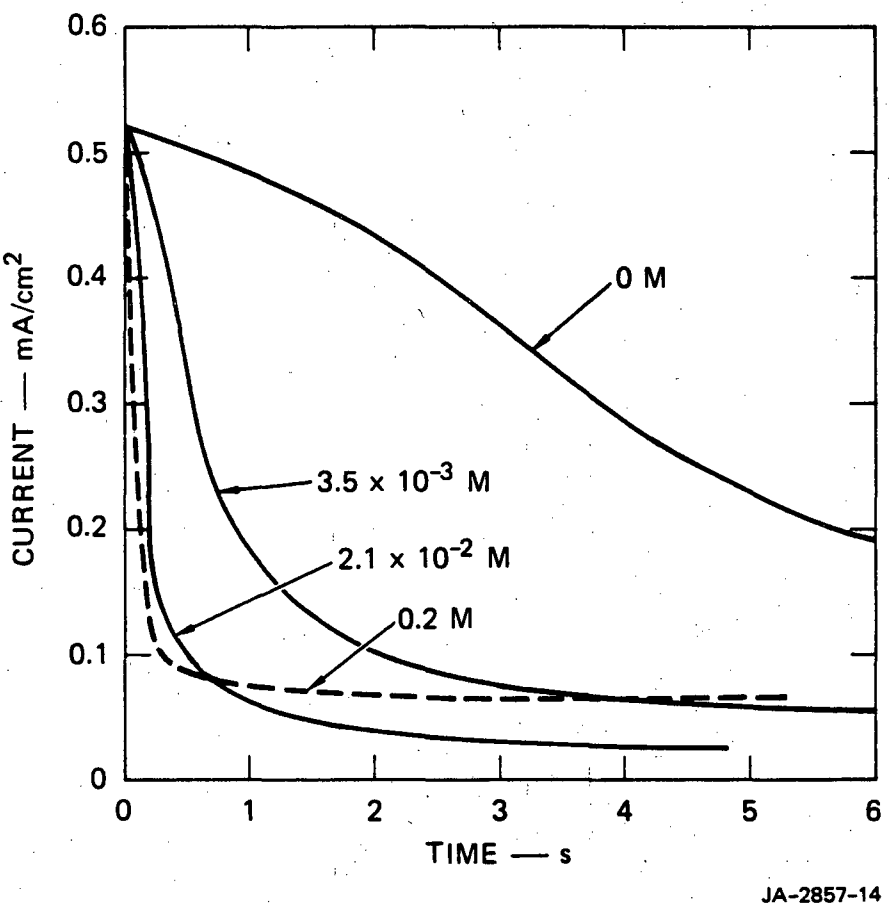

FIGURE 9 DECAY OF n-Si PHOTOCURRENT DUE TO OXIDE FORMATION

Solution 0.1 M $K_4Fe(CN)_6$, pH 5.5, voltage 0.7 V (SCE), NH_4F concentration as indicated.

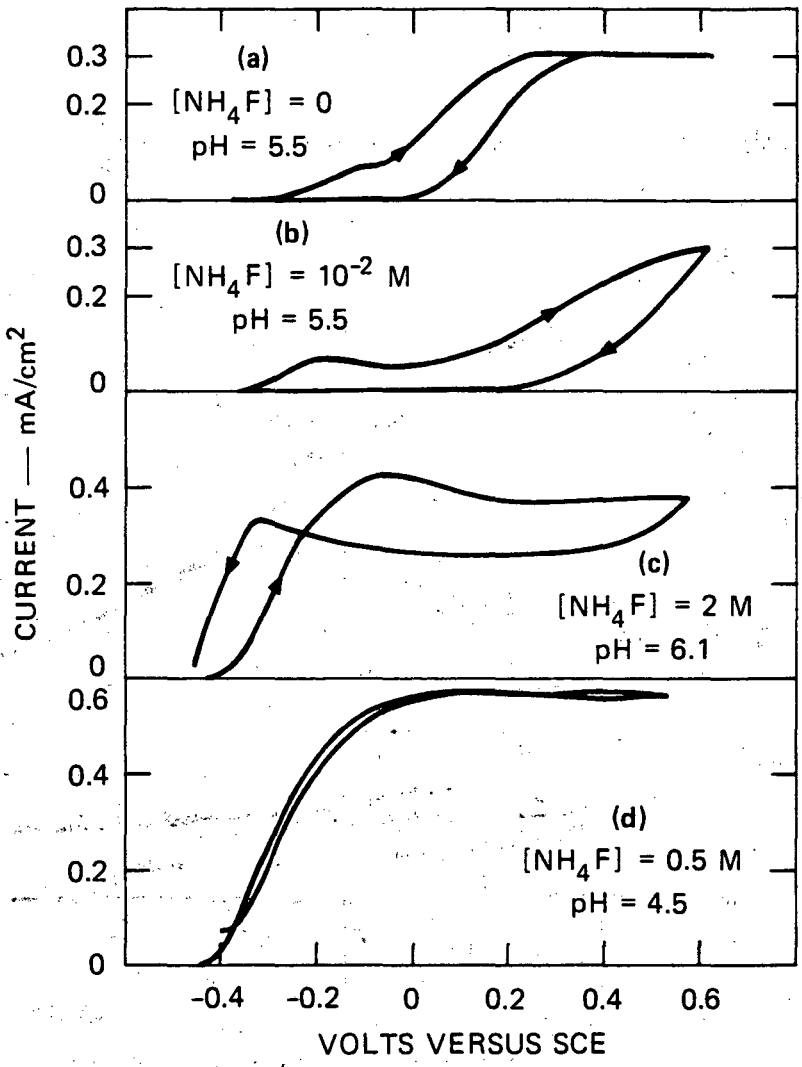

FIGURE 10 FIRST ANODIC SWEEP OF n-SILICON ELECTRODE UNDER ILLUMINATION

Aqueous solution, 0.2 M $K_4Fe(CN)_6$ + F^- as indicated.

presence of HF shifts the photocurrent onset potential anodically. When high concentrations of HF are present, the onset of photocurrent resumes its initial potential; however, the saturated photocurrent has increased twofold. Curves c and d of Fig. 10 illustrate this large increase in photocurrent.

Within the crystalline lattice, silicon is rigidly bonded through sp^3 hybridization. When one of the bonds is broken by interaction with HF, then the rigidity of the lattice decreases, allowing oxidation by hydroxide ions. Figure 11 illustrates factors that affect the photocurrent (aside from illumination intensity); the oxidation rate at the Si/SiO_x interface and the dissolution rate of the oxide at the SiO_2/solution interface. Under conditions of low HF concentration, the oxidation rate at the Si/SiO_x interface is high. The dissolution rate of oxide at the SiO_2/soln interface is comparatively lower. When the oxide becomes thick enough to inhibit the migration of HF and OH^- ions to the silicon surface, then the oxidation and dissolution rates will remain constant (equilibrate), resulting in a low saturation current. At high HF concentration, the dissolution rate of the oxide is very fast. When oxide thickness remains small, the ions have a short diffusion length. This increases the available HF and OH^- ion concentration at the Si/SiO_x interface. Then the photocurrent will be high, having contributions from oxide dissolution, surface oxidation and normal photocarrier - redox couple interaction.

Apparently, the ferrocyanide ion plays a conventional role in the charge transfer process, not catalyzing the oxidation process. That is, the system displayed low dark current corrosion, and the doubling in current could be attributed to the photoprocess. However, there are electrolyte systems where the doubling in current was directly related to dark current corrosion. In the presence of HF, TMPD catalyzes the dark corrosion of silicon by hole injection to the valence band (via interface states).

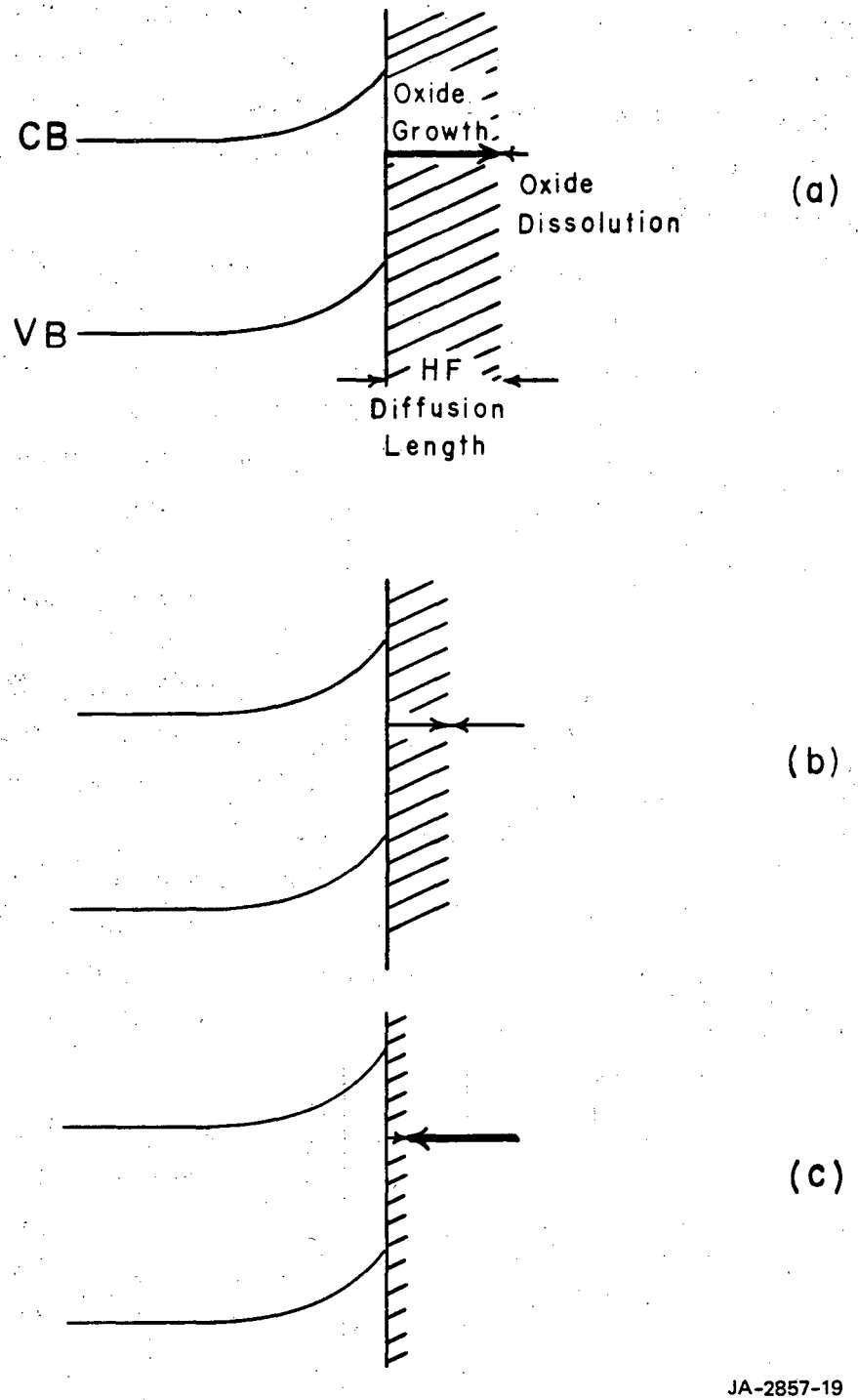

FIGURE 11 FACTORS AFFECTING THE PHOTOCURRENT

(a) Low HF concentration, high oxide growth rate, low photocurrent.
(b) Oxidation rate = dissolution rate, low saturation current.
(c) High HF concentration, high dissolution rate, high photocurrent.

III SOLAR CELL PERFORMANCE

Both p- and n-type silicon have been studied to determine what the problems would be in developing a photovoltaic battery. We solved the initial problem of sufficient photovoltage to drive the antimony battery (0.8-0.9 volts) by using the vanadium couple for the p-type silicon and the ferrocene/ferricenium couple for the n-type silicon electrode. Together, the p- and n-type electrodes can produce 1.13 V at open-circuit voltage (OCV) conditions, 0.51 OCV and 0.62 OCV, respectively. These systems were capable of stabilizing the silicon electrodes for a period of 0.5 hours with no more than a 10% decline in an initial current of 4.0 mA.

The major problem with this system is increasing the cell's efficiency where n-silicon is used, determined in part by a very low fill factor (ff = I x V at maximum power point).

There were two reasons for using the ferrocene/ferricenium redox couple in a nonaqueous solvent: first, a higher photovoltage could be obtained with a nonaqueous system than with an aqueous system; second, nonaqueous solvents should not be as conducive to photocorrosion on silicon as are aqueous solvents. Although the nonaqueous system has a low solution conductivity, this can be overcome with suitably arranged electrodes.

Several organic systems were studied to optimize the solar cell characteristic of silicon. The ferrocene/ferricenium in ethanol had favorable characteristics toward OCV and corrosion.[2] Unfortunately, the highest current densities obtainable here are no more than 0.83 mA/cm^2. One reason for the low current density is that ferrocene is not soluble in ethanol (0.07 M) in sufficient quantities to allow non-diffusion controlled current limitation. Adding a less polar solvent increases the concentration of ferrocene, allowing for a greater flux of reduced electrolyte species to the silicon/solution interface, and so increasing the allowable current.

Five nonaqueous solvent systems for the ferrocene/ferricenium couple, with ethanol as one of the two constituents, were examined for favorable solar cell characteristics. Table 2 lists the five solvent systems, in addition to neat ethanol, and the resultant short circuit current (I_{scc}) and OCV on one electrode. Ethanol was added to each system as a 1/3 volume constituent to maintain ferricenium solubility. Of the five solvent systems, methylene chloride/ethanol brought about the highest I_{SCC} (1.5 mA/cm^2) under the standard illumination intensity. The I_{scc} may be further enhanced by adding a few drops of acid such as HBF_4 or $HClO_4$. Silicon was stable against corrosion (oxide formation) for hours using this solvent system.

After finding a system with reasonable OCV and I_{scc}, our investigation concentrated on the parameters controlling the cell's efficiency. The fill factor of the silicon photoanode was far less than ideal. The SiO_2 layer on the silicon is the most probable cause of a low fill factor. We have concentrated on understanding an oxide film's influence on the fill factor. We have concluded both from experiment and theory that a thin oxide may benefit the solar cell characteristics, but a thick oxide will inevitably degrade the fill factor.

Table 2

NONAQUEOUS SOLVENT SYSTEMS

Solvent	$I_{scc}(mA/cm^2)$	OCV	Pt/SCE
EtOH[a]	0.69	0.46	0.44
CH_2Cl_2/EtOH	1.5	0.48	0.23
DMF[b]/EtOH	0.28	0.20	0.24
DMA[c]/EtOH	0.09	0.42	0.19
THF[d]/EtOH	0.18	0.44	0.34

[a]Support electrolyte was tetraethyl ammonium perchlorate.
[b]Dimethyl formamide.
[c]Dimethyl aniline.
[d]Tetrahydrofuran.

A. Experimental

1. Silicon/Silicon Dioxide Interface

There are two regions of oxide thickness to consider when determining the oxide's influence on solar cell characteristics. Region 1 includes oxides less than about 20 Å. Normally the surface oxide is 10-20 Å thick after a silicon electrode has been rinsed clean with both 6 M HF and distilled water, and exposed to air. Oxide layers thinner than this are very difficult to study in solution, while oxides thicker than this are relatively easy.

Region 1 is difficult to study because it is hard to avoid formation of the first layers of oxide, presumably because the silica formation is a spontaneous, highly exothermic reaction. The photogeneration of holes seems to accelerate this thermodynamically favored reaction, independent of the reduced species of a redox couple. After the oxide has attained the normal thickness, where dark oxidation processes at the Si/SiO_2 interface have been suppressed, then the solution redox couple can compete with further photoinduced oxide formation.

Figure 12 shows the variation of the solar cell characteristics as a function of oxide thickness. The measurements are made in CH_2Cl_2/EtOH with ferrocene/ferricinium as the couple, as described in Table 2. Very thin oxides (region 1) were obtained by wetting the silicon with a 12% HF solution and immersing it into the electrolyte with no exposure to air. By comparing the thin oxide curve with the air exposed sample, we suggest that curves 1 and 2 are in region 1, curves 3 and 4 are in region 2. In the same figure are the diode characteristics in the dark.

Two independent parameters control the solar cell characteristics: the dark current, and recombination at interface states. In other words, the cathodic current can be either the electron flow to the oxidizing agent in solution (also observed during measurements made in the dark), or the electron flow to interface states (a recombination process observed only during illumination). In region 1, where the oxide is very thin, the onset voltage of dark current processes is low. Electrons flow readily to ions in solution. The maximum photovoltage (where the electron flow compensates the hole flow to the surface) is influenced more by high

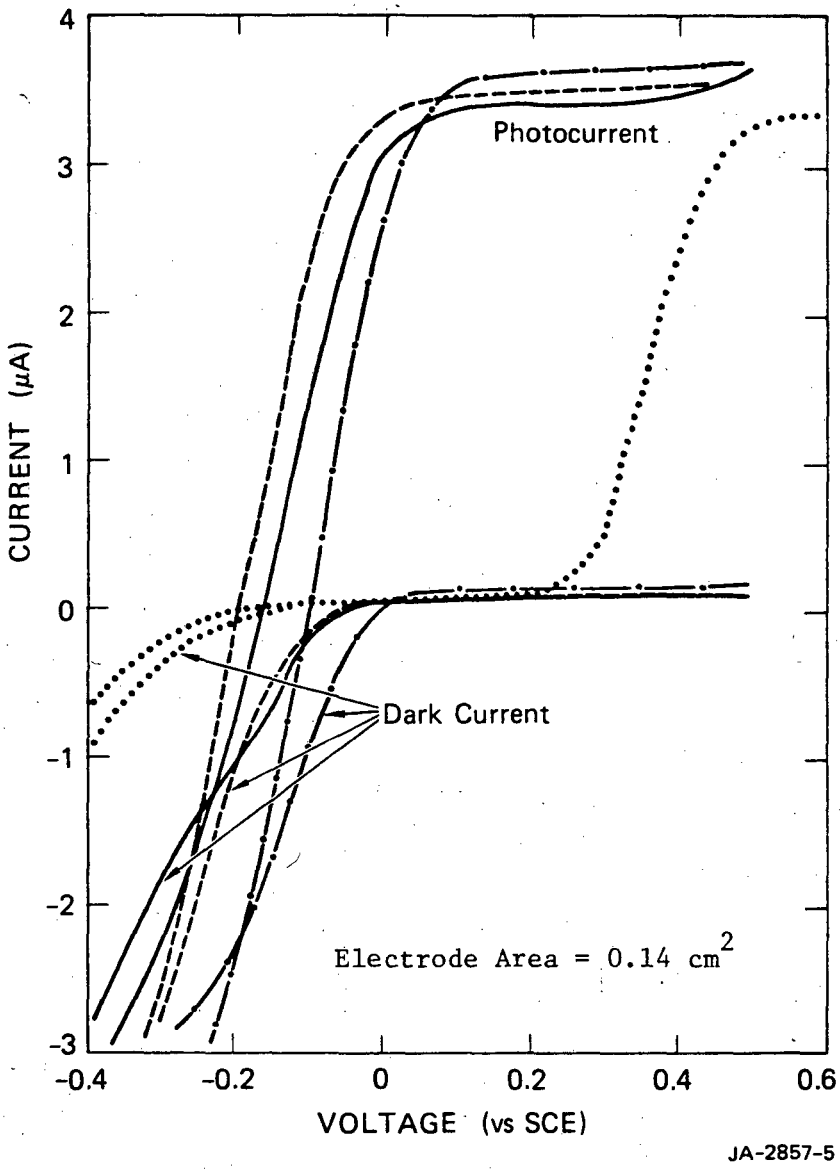

FIGURE 12 CURRENT VOLTAGE PLOT FOR n-Si AT VARIOUS OXIDE THICKNESSES

—•— Curve 1
- - - - - - Curve 2
——— Curve 3
••••••••• Curve 4

dark current processes than by the recombination at interface states. This condition is illustrated in curve 1, Fig. 12. As the oxide thickness increases, the electrons must tunnel through oxide and the dark current at a given voltage decreases. This shift is identified by a more negative onset voltage for the dark current in curve 2, Fig. 12. This dark current suppression allows for an increase OCV voltage in the photocurrent/voltage plot of curve 2, Fig. 1 where the hole density in interface states remains constant. An optimum condition occurs when the oxide thickness equals the "normal" oxide dimension identified by the transition from region 1 to region 2. When the oxide surpasses the optimum thickness (for an extreme case consider curve 4, Fig. 12) the oxide blocks all current flow, a significant voltage drop appears across the oxide, and interface state effects dominate dark current processes. Although the onset voltage of the dark current increases, the photovoltage decreases, as in curves 3 and 4, Fig. 12. The behavior is analyzed in the theory section to follow.

Similarly, the oxide thickness governs the flatband potential of the electrode. Figure 13 illustrates the relationship of the flatband potential in the dark to the oxide thickness. The flatband potential reaches a maximum near the optimum oxide thickness for V_{oc}. However, there is a problem in measuring capacitance-voltage plots with the very thin oxide (curve 1)--the slope, which should be the same as for the other curves, differs for curve 1.

The fill factor depends not only on oxide thickness but also on light intensity, as shown in Fig. 14. These results were taken with an oxide thickness corresponding approximately to that of curve 2, Fig. 12. The degradation of the fill factor as the light intensity increases is clear. We believe the effect of light on the fill factor is related to the varying voltage drop across the oxide, which in turn is related to the density of holes in interface states as a function of light intensity and voltage. At an intermediate voltage, e.g. -0.2 V, the density of holes occupying interface states at low light intensity is relatively low. The low density of holes, and subsequently the low voltage drop across the oxide (at constant oxide thickness), allows for a greater voltage drop across the semiconductor space charge region (greater band bending). The band bending induces more efficient electron-hole pair separation,

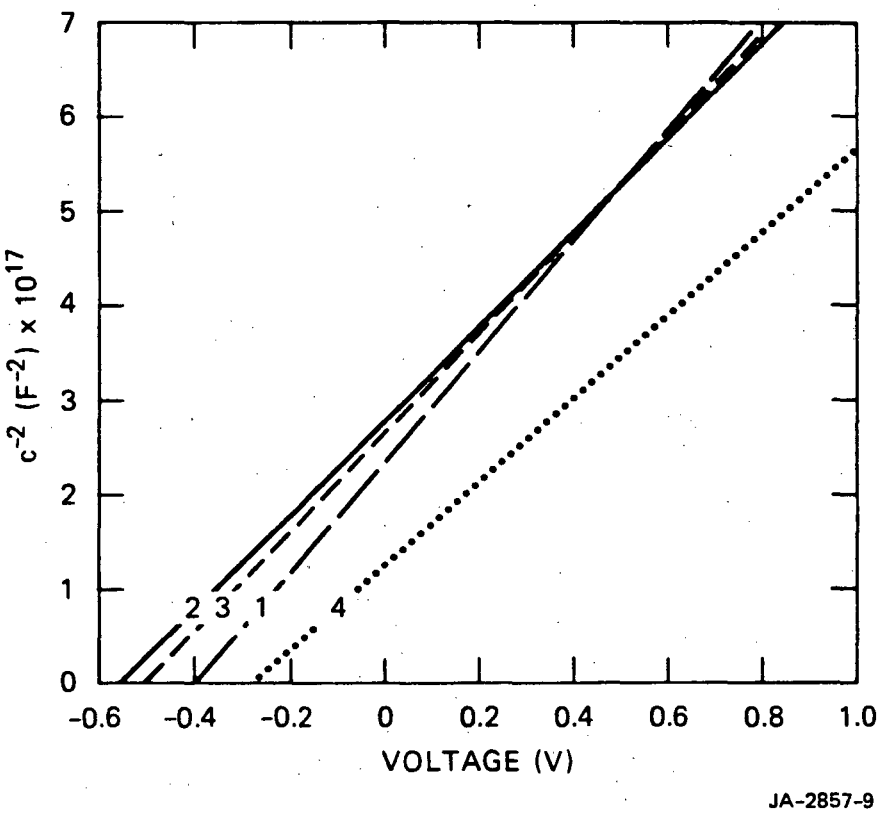

FIGURE 13 FLATBAND POTENTIAL DEPENDENCE ON OXIDE THICKNESS
Linear correlation coefficient $r^2 = 0.997$

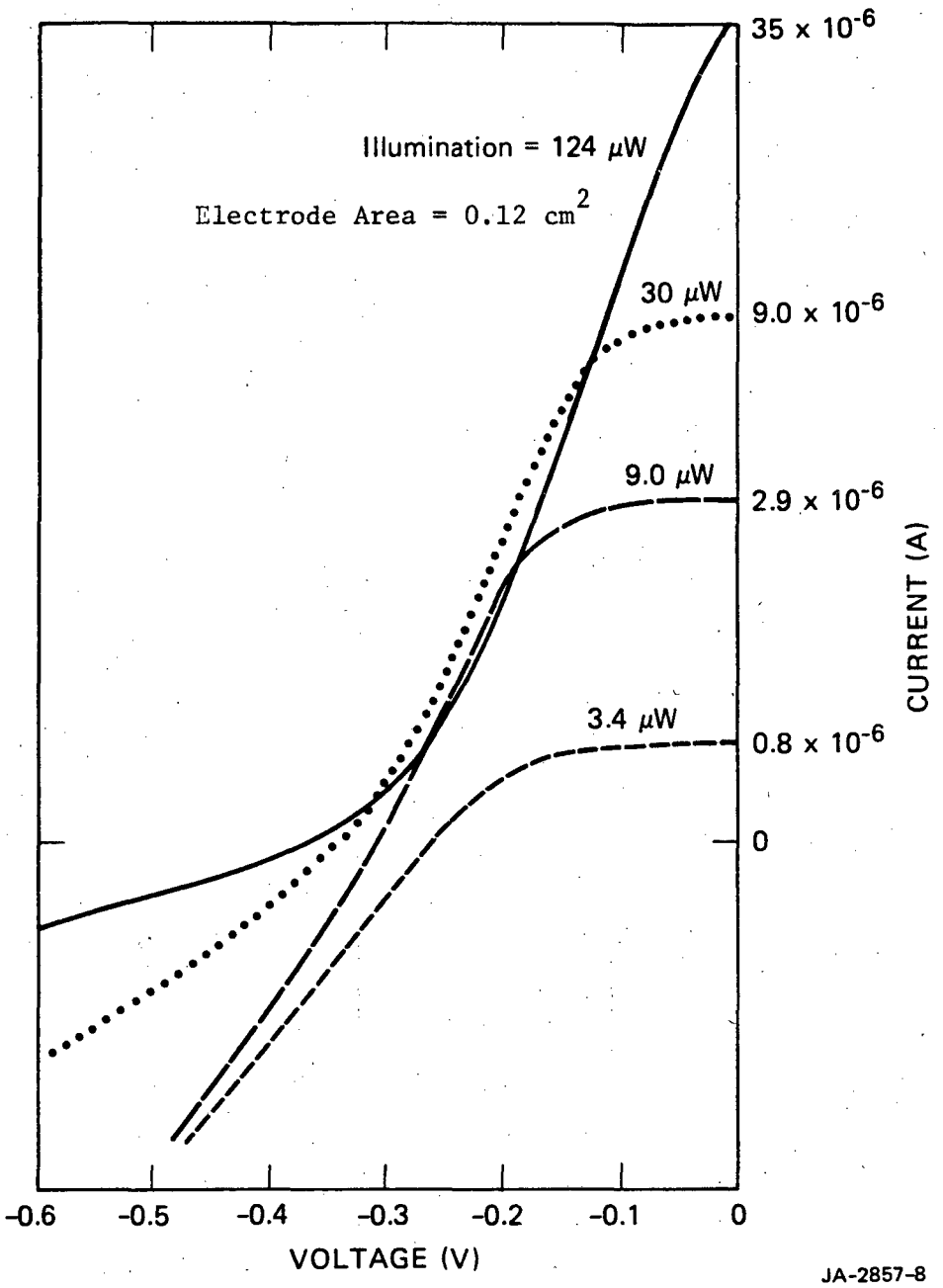

FIGURE 14 SOLAR CELL CHARACTERISTICS AS A FUNCTION OF LIGHT INTENSITY

resulting in a good fill factor. At high light intensity, where the hole density is high, a substantial fraction of the measured voltage appears across the oxide. Then at the highest light intensity of Fig. 7 (124 μW), we conclude that at V = -0.2 V much of the voltage appears across the oxide, the bands in the silicon are almost flat. A large percentage of the hole current then is lost to electron-hole recombination and the apparent fill factor is very low.

2. Cathodic Current Versus Electron Density at the Surface

The solar cell characteristics can be usefully described in terms of the electron density at the semiconductor surface. Through high frequency capacity measurements, the electron density at the surface is a derivable parameter.

The electron density at the surface is given by:

$$n_s = n_b \exp(-qV_s/kT) \tag{1}$$

where n_b is the bulk density, and V_s is the surface barrier. From Mott-Schottky plots, such as Fig. 13, the surface barrier is obtained from the capacity. The difference $V_m - V_{fb}$ is the surface barrier V_s (where V_m is the measured voltage, and V_{fb} is the flatband voltage) and in principle for all the curves of Fig. 13, a given capacity corresponds to the same $V_m - V_{fb}$. Unfortunately, some problems arise with very thin oxides (curve 1), as indicated by the nonparallel slope. In our analysis, we will ignore curve 1 and interpret all the capacity measurements as given a correct value for n_s as obtained from Equation (1) and using curves 2-4.

With this "measured" value of n_s, we can plot the cathodic current versus n_s in Fig. 15. The cathodic current is expected to be first order in the electron density at the surface and first order in the density of available states. Specifically one expects

$$J_c = J_{max} - J = a_1 n_s[Ox] \exp(-\alpha x_o) + a_2 n_s p_t \tag{2}$$

where J_{max} is the saturation anodic current obtained at high voltage when the cathodic current is zero (J_{max} = 0 in the dark with no anodic

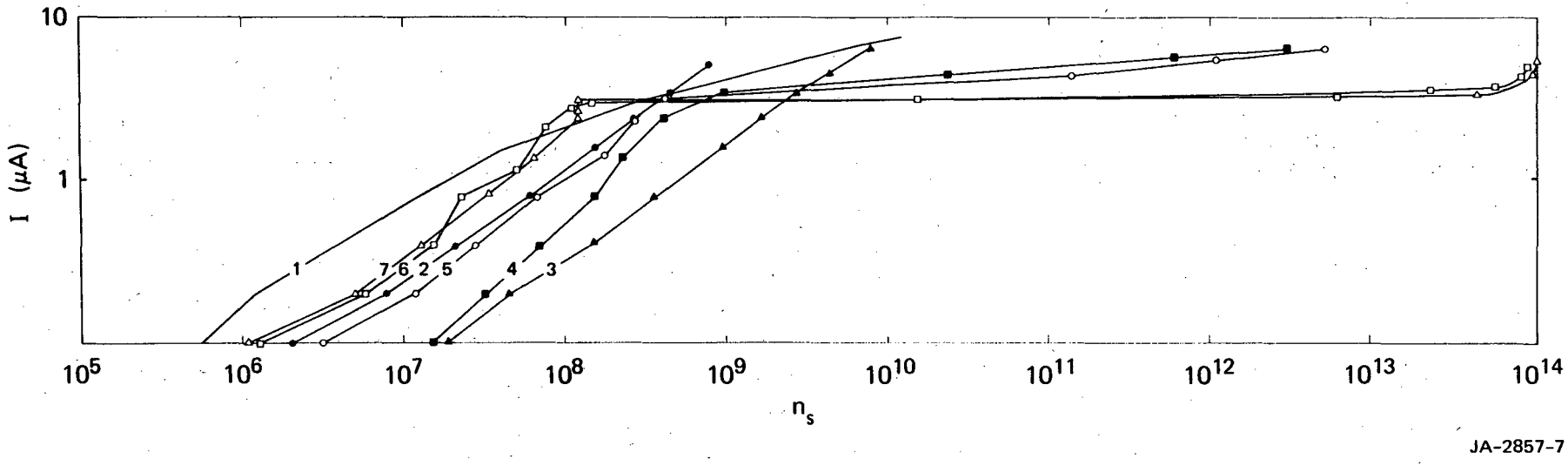

FIGURE 15 CURRENT (J_{max}-J) AS A FUNCTION OF THE NUMBER OF ELECTRONS AT THE SURFACE, n_s

current). J is the measured current. Thus the first equality in Equation (2) simply states that the net current, J, is the hole current J_{max} minus the cathodic current of interest, J_c. Then the second equality in Equation (2) says that the cathodic current has two components: one is the electron capture by the oxidizing agent Ox, which is modified by a tunneling factor $\exp(-\alpha x_o)$ where x_o is the oxide thickness; the other is the electron capture by interface states, which is proportional to n_s and to the density of unoccupied interface states, p_t.

Experimentally, if we plot the observed cathodic current, $J_{max} - J$, as a function of n_s (as measured by capacity), we have Fig. 15.The curves in Fig. 15 can be separated into two types, those corresponding to thin oxides and those corresponding to moderately thick oxides. With thin oxides, the cathodic current is simply proportional to n_s. With the thin oxides (curves 1-3) we expect the current to be dominated by the first term of Equation (2), namely, electron flow to the oxidizing agent. This term will dominate when x_o is small, because then the exponential factor approaches unity, and for both low and high n_s, the cathodic current is simply proportional to n_s with the proportionality constant $a_1[Ox] \exp(-\alpha x_o)$.

As the oxide becomes thicker, however, the exponential factor rapidly diminishes and the first term in the above expression becomes very small. Then at low n_s the second term begins to dominate. The current at a given n_s is much lower for these thick oxides, where the second term dominates, because the proportionality factor a_2pt is much less than $a_1[Ox]$. In this case, however, the current is limited. The cathodic current to interface states cannot be greater than the hole current to the interface states. Thus when the cathodic current reaches J_{max}, it becomes saturated. Mathematically, when the cathodic current reaches J_{max}, p_t rapidly approaches zero. However, as the voltage becomes even more cathodic, n_s increases exponentially. With increasing n_s, we finally reach a value at which the first term of Equation (2) becomes significant again, and J_c again begins to rise. The shift in the value of n_s needed for a given current is directly related to the factor $\exp(-\alpha x_o)$ in the equation for J_c. This plateau in J_c at low n_s, followed by an increase in J_c as n_s becomes very large, is seen in curves 4-7.

From these data, a clear understanding can be obtained of the behavior of the important cathodic current that limits the solar cell efficiency. We can determine the rate constants for the electron capture by the oxidizing agent and by interface states, and we can demonstrate the influence of the oxide layer on the tunneling process. This type of analysis is discussed further in the theory section.

Attempts to avoid the problems of the oxide layer have taken two directions. We have tried to minimize the interface state density, and we have tried to minimize the oxide thickness.

To minimize the interface state density we have borrowed the hydrogenation technique from integrated circuit technology. However, this has not proved effective. It may be that with our thin oxides (~ 25 Å) the oxides react too rapidly with residual water. In any case no significant improvement in interface state density has been observed. the interface state density has been measured (using quasi-static techniques) to provide better monitoring of such experiments.

The other technique is to maintain a thin oxide by introducing a corrosive material (HF) into the solvent. This has met with little success because we found that the effectiveness of the stabilizing agents was degraded in the presence of HF.

B. Theory

Although several papers have analyzed the current/voltage characteristics of a semiconductor electrode under illumination,[3-6] the case with a film present has not been discussed. As will be shown below, a surface film (a condition often expected for an electrode) can dramatically affect the solar cell characteristics, particularly the fill factor. Of course, if the film is completely insulating the current is zero; the cases of practical interest are those where the film is present but thin enough for electron tunneling, or where the film is conductive enough to pass current. We emphasize the former because we are interested in silicon. The qualitative features should remain equally true in the case of the conducting film.

The experimental results discussed in the preceding sections can be explained in detail by simply assuming the presence of a tunnelable oxide, and assuming very normal electrode behavior. Thus we will show cases, comparable to observation, where we predict a very low apparent fill factor and cases where we predict that the OCV becomes more negative or positive with increasing oxide thickness. In particular, we will show cases where a thin oxide benefits the solar cell efficiency. The last is particularly important in discussing MIS solar cells.

1. Analysis

A model of the surface shown in Fig. 16 will be used. The model is somewhat distorted dimensionally--the band bending shown for the silicon should span about 1000-2000 Å , the oxide thickness is 0-50 Å. Also, the conduction and valence band in the SiO_2 should be further from the band edges in the silicon. However, the model as drawn shows the important parameters.

We assume the hole flux to the surface is distributed between hole capture by interface states and hole capture by reducing agents in solution. We assume the hole flux to the surface is independent of the applied potential. This means we are assuming that the diffusion length is much greater than the space charge thickness, and that the hole emission into the valence band by interface states or by oxidizing agents in solution is negligible. Then

$$J_{sat} = qK'_p p_s[Red] \exp(-\alpha x_o) + qK_p p_s(N_t - p_t) \qquad (3)$$

describes the hole flux, J_{sat}. The subscript "sat" refers to the saturation hole current at high reverse bias, which (by the assumption above) is the hole flux. The first term in Equation (3) represents hole capture on reducing agents in solution, described as first order in the hole density at the surface and first order in the effective surface concentration of reducing agent concentration (the concentratin in solution times an effective tunneling distance). The term is also proportional to a rate constant K'_p and proportional to a tunneling factor describing tunneling of carriers through the oxide of thickness x_o, where α is a

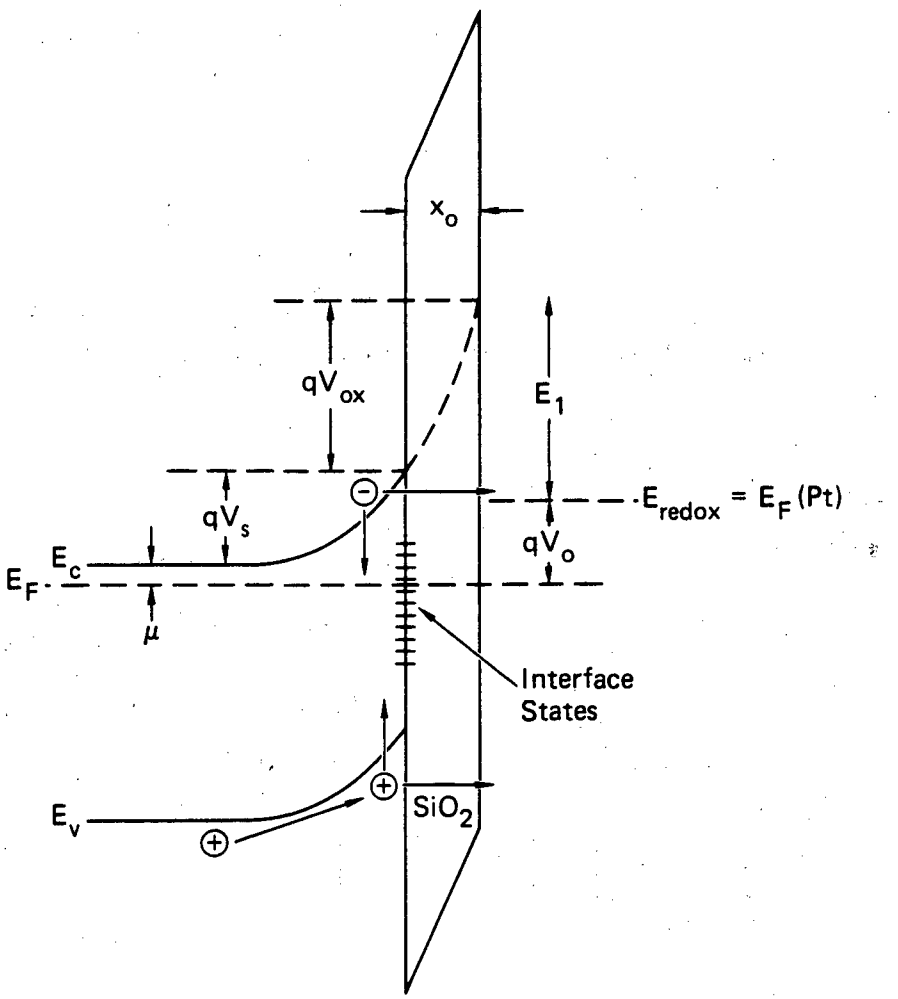

JA-2857-10

FIGURE 16 BAND MODEL FOR THE SILICON ELECTRODE

Electrons or photo-produced holes reaching the surface can be either captured by interface states or can funnel to ions in solution as indicated by the arrows.

constant. The second term of Equation (3), the hole capture by interface states, is also described as first order in hole density and first order in the interface states ($N_t - p_t$). Here N_t is the total interface state density, p_t the hole concentration, and K_p is a rate constant. We ignore corrosion mechanisms, and we ignore the change in the effective [Red] caused by a voltage across the oxide shifting the Gaussian distribution of energy levels in solution relative to the valence band of silicon.[7]

We have an analogous expression for electron capture

$$J_c = qn_b \exp(-\beta V_s) \{K_n'[Ox] \exp(-\alpha x_o) + K_n p_t\} \tag{4}$$

which describes the cathodic current to oxidizing agents in solution (first term) and to interface states (second term). The rates are first order in the density of electrons at the surface, $n_b \exp(-\beta V_s)$ (with n_b the bulk density, $\beta = q/kT$, and V_s the surface barrier). The rates are also first order in the effective density of unoccupied levels, where in the first term [Ox] is the density (per unit area) of available ions in solution, and in the second term p_t is the density of unoccupied interface states. The capture of carriers by ions in solution is lowered by the tunneling factor, $\exp(-\alpha x_o)$, assumed to be the same factor as in hole capture.

In steady state, the electron capture rate and hole capture rate on the interface states are equal:

$$K_p p_s (N_t - p_t) = K_n p_t n_b \exp(-\beta V_s) \tag{5}$$

Now J_{sat} is a parameter to be specified, so the only variables in Equations (3) and (4) are V_s, p_t, and p_s. With Equations (3) and (4) we can eliminate p_s, obtaining an expression for p_t in terms of V_s:

$$N_t - p_t = -(1/2)\, b_2 \{1 \pm (1 + 4b_1 N_t/b_2^2)\}^{1/2} \tag{6}$$

where the sign is chosen so that $o < p_t < N_t$, and where

$$b_1 = (K_p'/K_p)[Red] \exp(-\alpha x_o) \tag{7}$$

$$b_2 = b_1 - N_t + J_{sat}/q\ K_n n_b\ \exp(-\beta V_s) \tag{8}$$

Now we assume that the voltage V_{ox} in Fig. 16 arises primarily because of charge in the interface states (and the counter-charge in the solution), neglecting the charge in the space charge region of the semiconductor. The charge in the space charge region will be on the order of 10^{11} q/cm^2, whereas we are assuming more than 10^{12}/cm^2 interface states. Then

$$V_{ox} = (qx_o/\kappa\varepsilon_o)\ (p_t - p_{to}) \tag{9}$$

where p_{to} represents the hole density on the interface states when the net interface state charge is zero.

With the equation

$$V_o + E_1 - V_s - \mu - V_{ox} = 0 \tag{10}$$

obtained by inspecting Fig. 16 we obtain

$$V_o + E_1 - V_s - \mu - (qx_o/\kappa\varepsilon_o)\ (p_t - p_{to}) = 0 \tag{11}$$

The parameter E_1 is $E_c - E_{redox}$ when $x_o = 0$. This is not a constant because $E_{redox} = E_o + kT\ \ln[Red]/[Ox]$ depends on [Red] and [Ox]. Now inserting Equation (6) into Equation (11), we have an equation in V_s that can be solved to give V_s as a function of V_o, the measured voltage. Then from Equation (6) we obtain p_t, from Equation (9) we obtain V_{ox}, and from Equation (5) we obtain p_s, all expressed as a function of V_o. We can then solve for the current as a function of V_o.

The current actually measured is the difference between the hole capture rate in the solution and the electron capture rate in the solution:

$$J = qK_p'[Red]p_s\ \exp(-\alpha x_o) - qK_n'[Ox]n_b\ \exp(-\beta V_s - \alpha x_o) \tag{12}$$

Because in Equation (11) the variable V_s appears both as a linear factor and in the exponent, an analytic solution to Equation 11 is not possible.

Below we discuss various computer solutions, showing the strong effect of the oxide in the apparent fill factor of the solar cell.

2. Open Circuit Voltage (OCV)

The equations above can be solved analytically for the OCV circuit by setting Equation (12) equal to zero. This calculation can be used to predict the conditions under which V_{oc} increases with decreasing x_o (becomes more negative) and the conditions under which V_{oc} decreases with increasing x_o.

Inserting Equation (12) (with J = 0) into Equation (3), we immediately obtain an expression for p_t at open circuit:

$$p_t = N_t/(1 + \gamma), \tag{13}$$

with

$$\gamma = K_n K_p'([Red]/K_n' K_p)[Ox] \tag{14}$$

Inserting Equation (13) in Equation (3) (yielding p_s), Equation (5) (yielding V_s), and Equation (9) (yielding V_{ox}), Equation (11) can be solved for $V_o = V_{oc}$:

$$V_{oc} = -E_1 + \mu + \beta^{-1} \ln\{a_2^{-1}(K_n' K_n^{-1}[Ox]e^{-\alpha x_o} + [1+ \gamma^{-1}]N_t)\}$$

$$+ (qx_o/\kappa\varepsilon_o)(N_t/[1 + \gamma] - p_{to}) \tag{15}$$

When the second term under the log is greater than the first term, namely, at high x_o, the change in V_{oc} with x_o is given by the last term of Equation (15). In all cases, the value of dV_{oc}/dx_o can be negative or positive depending on the value of γ and other factors. As will be observed in the numerical examples to follow, this can substantially increase the solar cell efficiency for small x_o, that is, a thin film can improve V_{oc} and hence the solar cell efficiency. Such an effect is, of course, well known in MIS solar cells.

3. Numerical Examples

In Figure 17 we show example solutions for the above equations, showing the predicted current/voltage characteristics of an oxide-covered silicon solar cell. Reasonable values for the parameters are used:

$$K'_n = K'_p = K_{p_8} = 10^{-7} \text{ cm}^3/\text{sec},$$
$$K'_p = 5 \times 10^{8} \text{ cm}^3/\text{sec}$$
$$E_1 = 0.8 \text{ ev}, \ \mu = 0.1 \text{ eV}$$
$$N_t = 2 \times 10^{12} \text{ cm}^{-2}$$
$$p_{to} = 10^{12} \text{ cm}^{-2}$$
$$\alpha = 2 \times 10^{7} \text{ cm}^{-1}$$
$$n_b = 3 \times 10^{15} \text{ cm}^{-3},$$
$$J_{sat} = 10^{-4} \text{ A/cm}^2$$
$$[\text{Red}] = 4 \times 10^{13} \text{ cm}^{-2} \text{ (just less than 1 molar)}$$
$$[\text{Ox}] = 10^{13} \text{ cm}^{-2}.$$

The oxide thickness x_o is varied from 0 to 50 Å. The values for the parameters are chosen to match more or less the values estimated for the silicon used to obtain the data of Fig. 12. Thus the form of the curves in Fig. 17 can be compared to the form of the curves in Fig. 12. The theory obviously provides the same type of curves that are experimentally observed.

In Fig. 18 are curves of the cathodic current a function of electron density at the surface for the same parameters as used in Fig. 17. These can be compared with the experimental curves of Fig. 15. Again the general form of the curves is quite similar.

The conclusion from this modeling is that the major part of the problem with fill factor in the silicon electrode can be traced directly to the presence of the oxide and to the interface states between the oxide and the silicon.

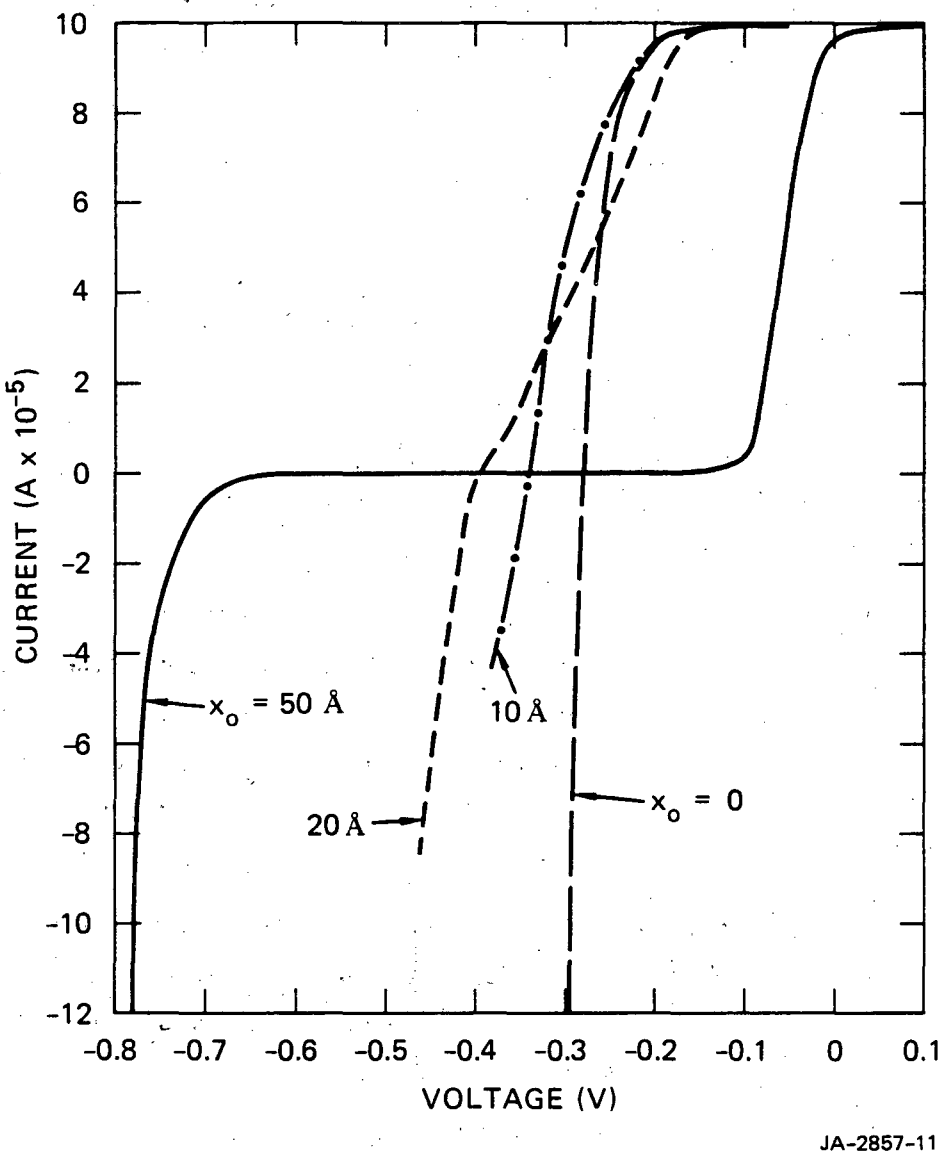

FIGURE 17 THEORETICAL CURRENT/VOLTAGE CHARACTERISTICS FOR CELL WITH PARAMETERS DESIGNATED AS DESCRIBED IN THE TEXT

Then these theoretical curves should be compared to the experimental photocurrent curves of Figure 1.

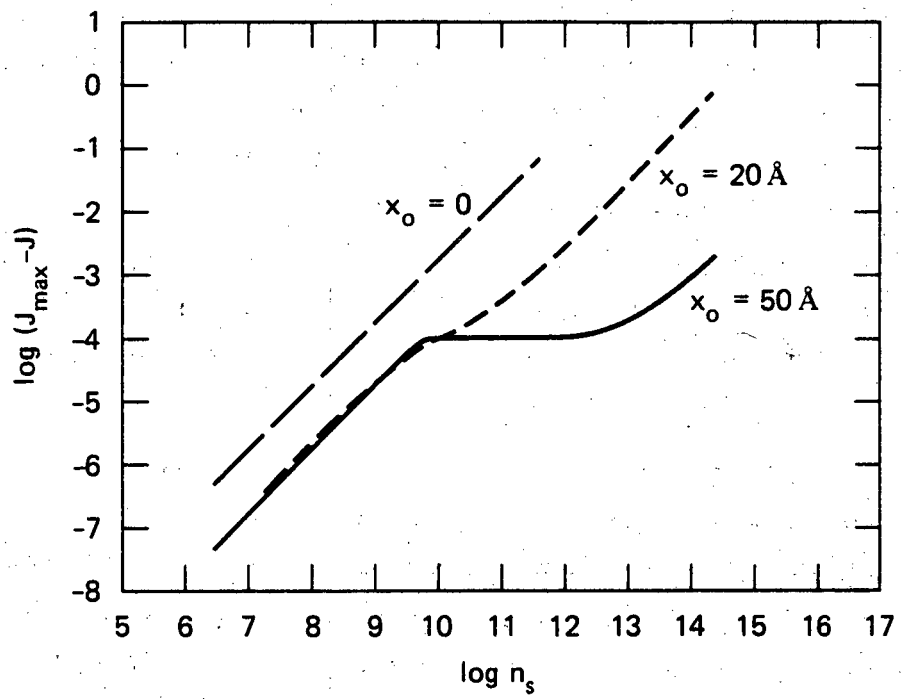

FIGURE 18 CATHODIC CURRENT (J_{max}-J) VERSUS SURFACE ELECTRON DENSITY WITH VARIOUS OXIDE THICKNESSES

The parameters used are described in the text. These curves should be compared to the experimental curves of Figure 4.

IV SURFACE TREATMENTS

Earlier results suggest than an oxide layer on n- or p-type silicon in excess of about 20 Å is detrimental to the use of this material in photoelectrochemical cells. Aside from the common problem of the normal oxide on both n- and p-type silicon, the problems associated with running each type at a high efficiency level are different. n-Type silicon is much more susceptible to corrosion because of photo-generated holes at the surface. Bare n-type silicon cannot be used in an aqueous system because the combination of relatively high hole concentration and an unlimited supply of oxygen (from H_2O) promotes rapid formation of insulating SiO_2. p-Type silicon has a much lower effective concentration of holes at the surface. For this reason, p-type silicon may be used in aqueous redox systems.

An organic solvent can be used to minimize the corrosion of n-type silicon. When a proper organic redox couple is used, a high photovoltage can be obtained, as is the case with ferrocene/ferricenium in a methylene chloride ($MeCl_2$) ethanol (EtOH) mixed solvent. Unfortunately, this nonaqueous system has slower charge transfer kinetics than a comparable aqueous system. Slower charge transfer between the redox couple in solution and the semiconductor surface limits the current. The maximum short circuit current we have demonstrated with the ferrocene/ferricenium nonaqueous system has been under 1 mA/cm^2.

Several methods have been examined to increase the efficiency of the silicon electrodes. The first was heat treating the electrodes under argon or hydrogen gas. The second involves making p-n silicon and plating a thin layer of platinum on the surface. The third uses poly-vinylcarbazole as a protective coating on the surface of the photoanode.

A. High Temperature Treatments

It was concluded that the low efficiency of the silicon photoanodes was due to a high density of interface states at the Si/SiO_x junction. These interface states are attributed to unsaturated silicon bonds or to surface silicon covalently bonded to H or OH radicals. The charge in the interface states leads to a voltage across the silica layer, degrading the fill factor of the solar cell.

The interface state density was determined as a function of oxide thickness, because a principal problem with silicon PECs was oxide growth. It was found that as the anodic oxide increases, the density of interface states increases. This means that a thick oxide can be doubly detrimental, being an effective insulator as well.

Methods to decrease the interface state density were investigated. Two surface treatments for lowering the interface state density were studied. The first was simply an attempt to treat the unsaturated silicon bonds by thermal rearrangement of the oxide crystal lattice. A thermal rearrangement might increase the bonded oxygen-silicon density and leave fewer silicon nonbonding levels. Thermal treatment was expected also to dehydrate the silica. The treatment consisted of heating the crystal (which has an oxide of 10-15 Å) to 300°C for 15 min. under an argon atmosphere. The purpose of the argon atmosphere was to keep the native oxide from growing too thick to pass charge. Using capacitance/voltage detection methods, we found no decrease in interface state density. Also, no improvement in conversion efficiency was found following this treatment.

The second method of treatment follows the efforts applied to integrated circuits (using MOSFETs) and to MIS solar devices. This involved hydrogenation of the Si/SiO_x interface region by heating the samples at 300°C, 650°C and 1000°C for 30 and 60 min under a hydrogen atmosphere. Hydrogen diffusing through the oxide reacts with the unsaturated bonds on silicon, lowering the interface state density. From capacitance/voltage experiments we determined that the interface state density could be lowered by a factor of 2, in the range of 10^{11}

cm^{-2} $(eV)^{-1}$ states. Unfortunately, the prescribed treatment of hydrogenation did not increase the efficiency of the device. Like solid state devices, a substantial increase in efficiency may not be obtained until the interface state density approaches $10^{10}/cm^2$ (eV). Attempts to reach this limit with the liquid junction device have been unsuccessful.

B. p-n Silicon Electrode

We have attempted another approach to electrode stabilization using a thin platinum coating on a p-n junction cell. The platinum coating inhibits the corrosion of silicon in an aqueous solution by physically separating the silicon and the electrolyte. A layer of platinum, estimated to be between 60 to 140 Å, was deposited on samples using a sputtering device. About 100 Å seemed to be an optimal thickness. Corrosion still takes place with the metal coating. Although a thicker coating would more effectively suppress the corrosion, it also adsorbs light. Figure 19 illustrates a 2.5% efficient cell having the optimal metal coating. Efficient solar cell characteristics can be attributed to the band bending in the n-type induced by p-type and fast charge transfer across the interface with an aqueous solution of 0.1 M Fe (II, III) EDTA at pH 5.5. Other samples were examined to determine whether or not diffusing the platinum into the silicon surface would favorably affect efficiency. There was no evidence that annealing platinum coated p-n silicon at 800°C for 10-20 min had any effect on the overall charge transfer rate. What is more important is the p-type junction depth and the surface oxide thickness. We observed large differences in conversion efficiency with many samples. However, no attempt was made to determine the optimum junction depth of p-type material.

C. Polymer Coatings

Preliminary work on surface stabilization using poly-vinylcarbazole was begun. Poly-vinylcarbazole is known to be a reasonably good hole conductor and the conductivity can be increased by adding dopants. The

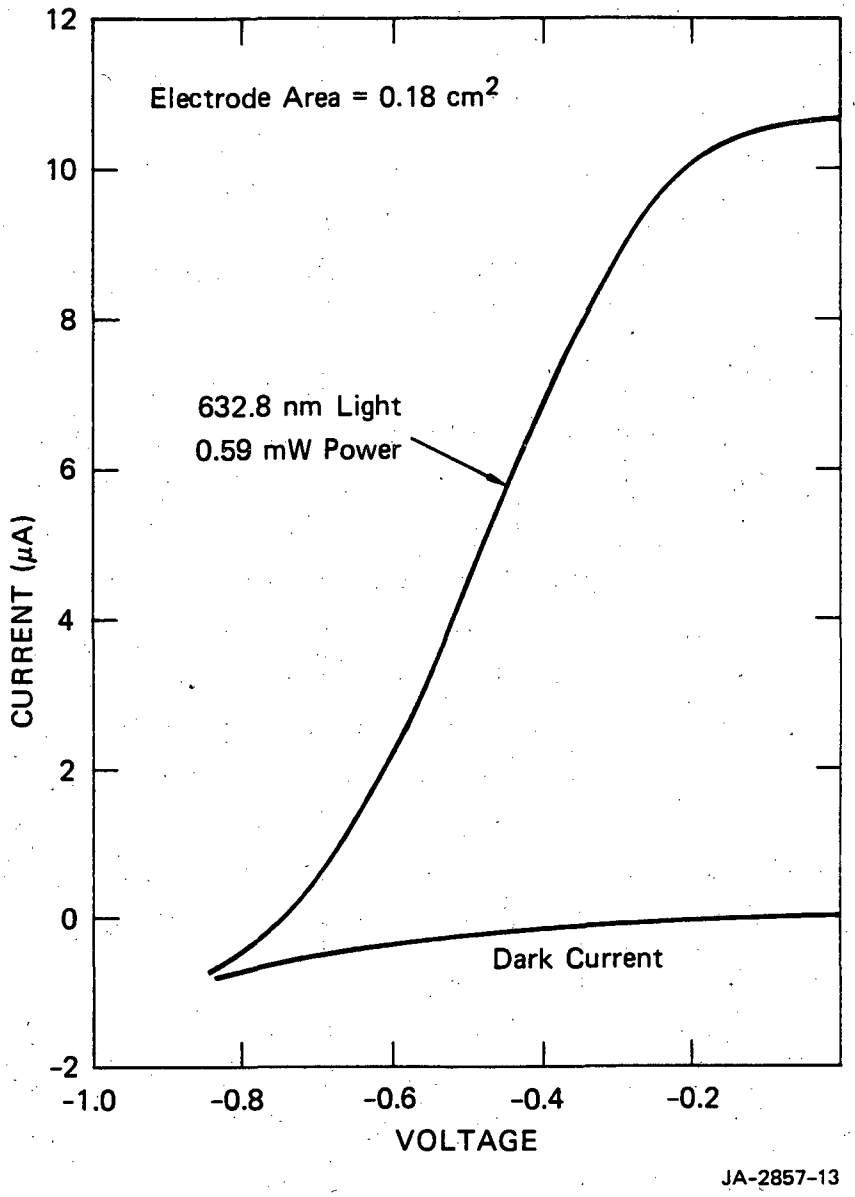

FIGURE 19 POWER CURVE FOR pnSi IN 0.1 M Fe(II, III) EDTA, pH 5.5

Surface of electrode has ≈ 100 Å of platinum covering the p-type silicon

hole mobility can be decreased by the addition of trinitrofluorenone (TNF). At sufficiently high TNF concentrations, electrons will dominate the conductivity. However, for the purposes of stabilizing n-type silicon, high hole mobility would be favorable and can be accomplished by adding compounds like triphenyl amine. The hole transport mechanism is thought to occur by intermolecular hopping.[8]

It was thought that the conducting energy levels could be adjusted within the polymer to correlate with the semiconductor and redox couple. Experiments here describe solar cell characteristics of n-silicon with neat poly-vinylcarbazole and doped polymer on the surface.

Figure 20 illustrates current-voltage characteristics for a silicon photoanode with and without the polymer coating. Each coating was applied by placing a drop of toluene solvent, containing the polymer, onto the electrode surface. Taking the density of the polymer to be 1.185 g/cc[9] we estimated that the coating was approximately 2000 $\mathring{A}$ thick. The polymer was then dried in an oven at 100°C for one-half hour. Electrode characteristics with an undoped polymer coating are given by curve 1. Curves 2 and 3 illustrate greater hole conductivity through the polymer, having 8% and 83% mole fraction of triphenyl amine dopant respectively. Clearly, as the mole fraction of polymer dopant was increased the conductivity increased. However, there was no advantage in doping above 83% mole fraction, as further improvement in the photocurrent was negligible.

Experiments were conducted to determine the effect of various redox couples on the charge transfer properties of the poly-vinylcarbazole. These aqueous and one nonaqueous redox couples were tested with heavily doped polymer coated photoanodes. Figure 21 illustrates the current-voltage characteristics in 0.1 M I^-_3. Although the photocurrent onset potential has decreased, the polymer was capable of passing a larger current than was possible for a bare surface undergoing photoanodic oxidation. The most responsive redox couple to the polymer was iron cyanide. Figure 22 shows an improvement in the photocurrent onset potential. In all cases the dark current was suppressed. For both the

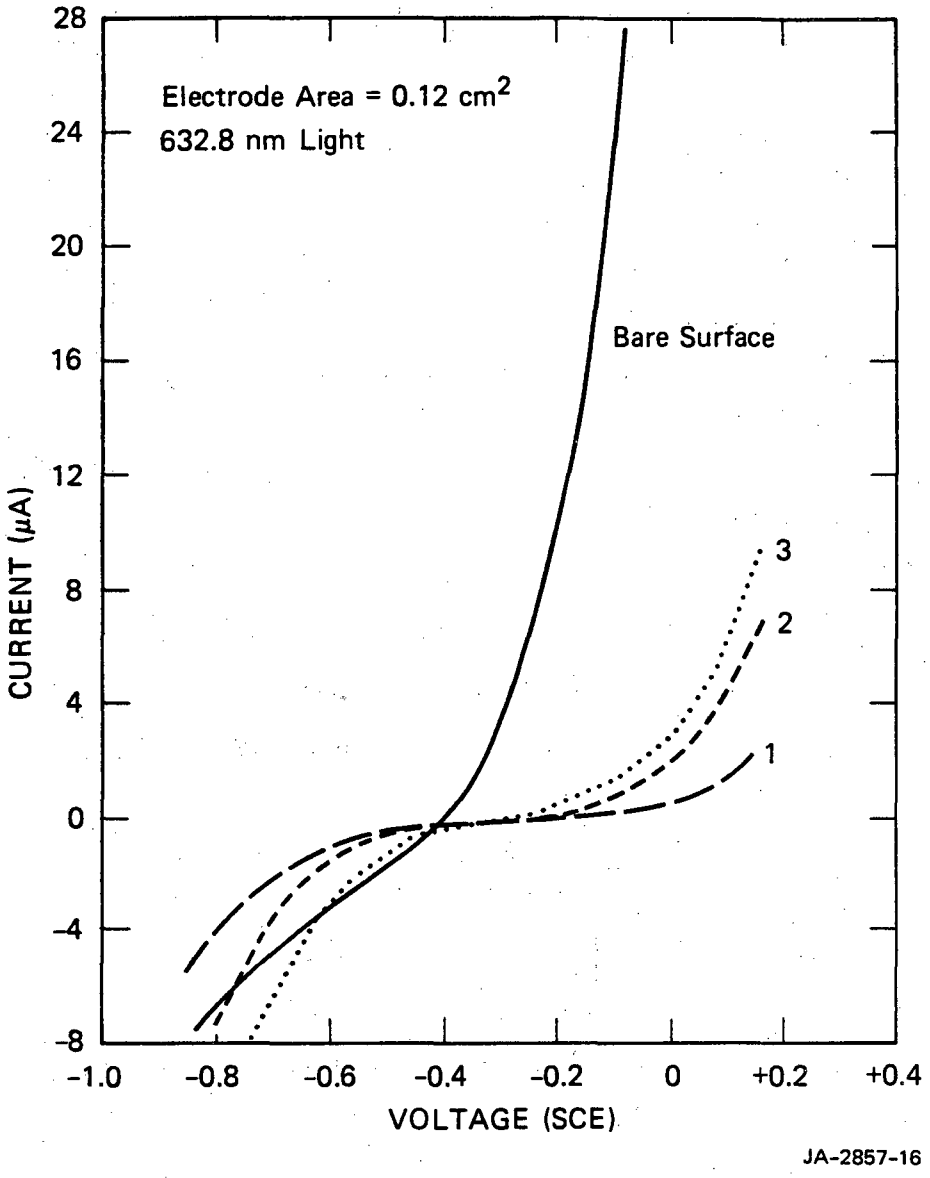

FIGURE 20 CURRENT-VOLTAGE CURVES FOR n-TYPE SILICON IN 0.1 M $Fe(EDTA)^{III/II}$

1. Surface coated with poly-vinylcarbazole.
2. Poly-vinylcarbazole with 8% mole fraction triphenyl amine.
3. Poly-vinylcarbazole with 83% mole fraction triphenyl amine.

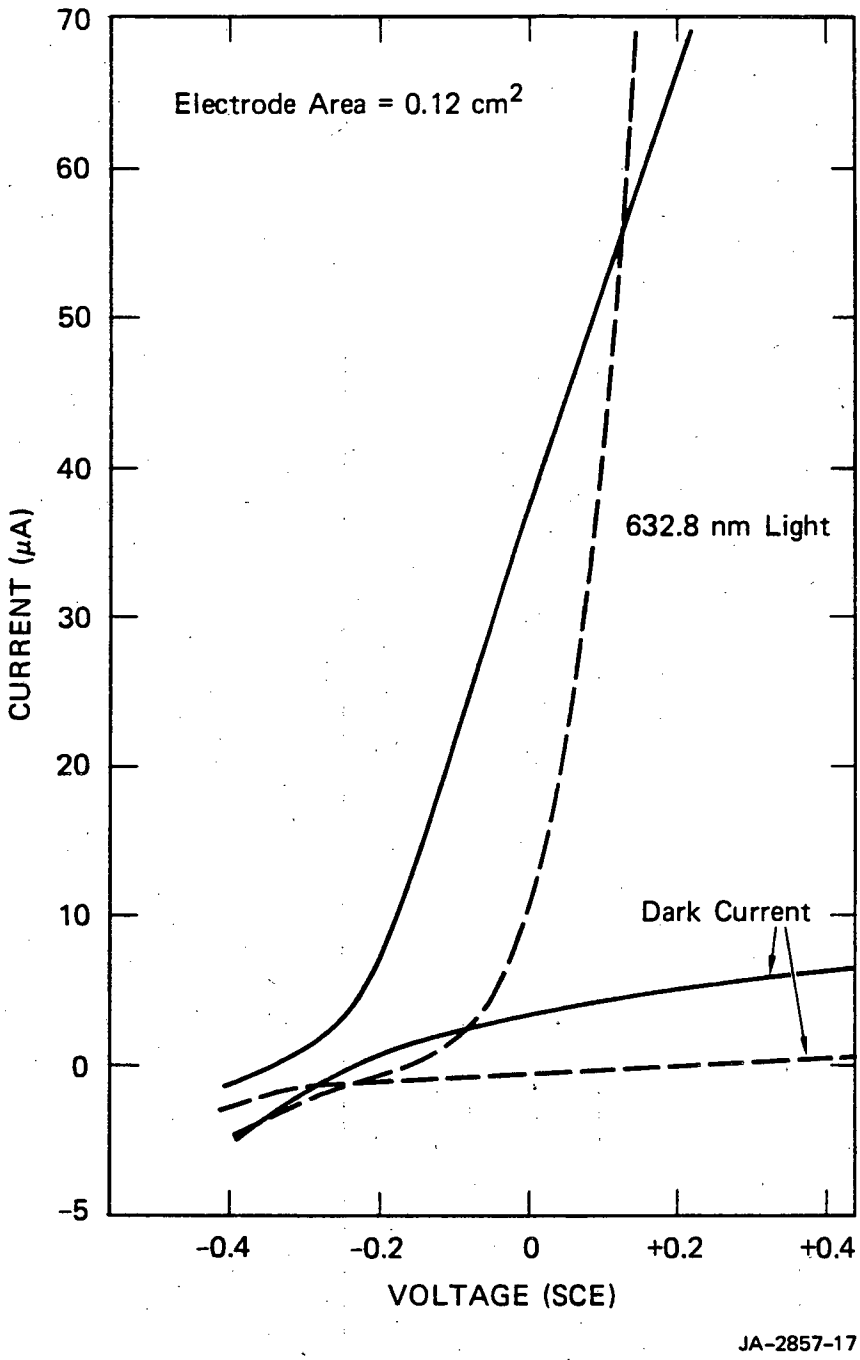

FIGURE 21 POWER CURVES FOR n-Si IN 0.1 M I_3^-

(———) Clean surface after being washed with 12% HF.
(– – –) Surface of electrode covered with poly-vinylcarbazole doped with triphenyl amine.

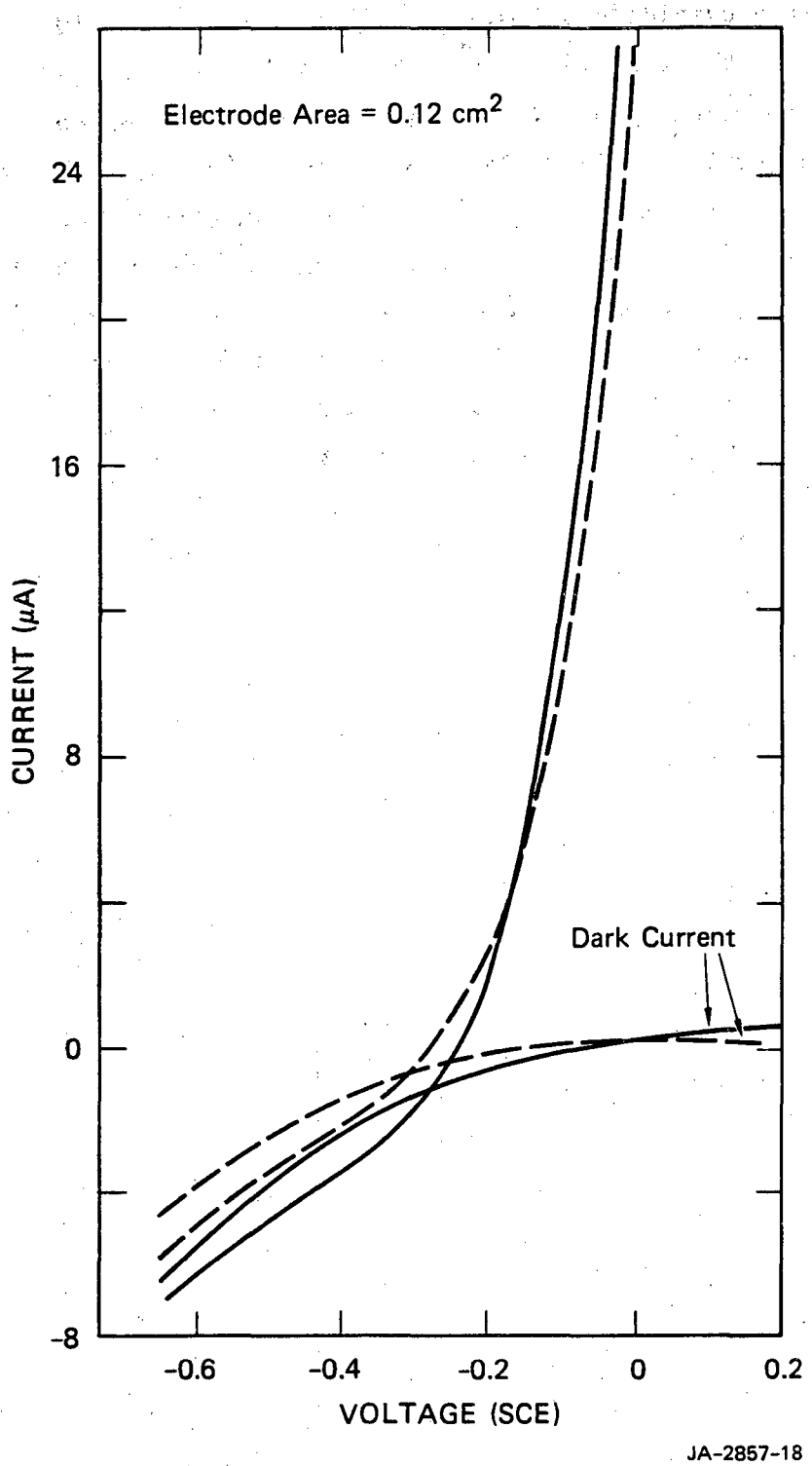

FIGURE 22 POWER CURVES FOR n-Si IN 0.1 M $Fe(CN)_6^{4-}$, 0.1 M $Fe(CN)_6^{3-}$
(———) Clean surface after being washed with 12% HF.
(— — —) Electrode surface covered with poly-vinylcarbazole doped with triphenyl amine.

triiodide and iron cyanide couples, the anode experienced a 10% drop in SCC during the first 5 minutes of operation at about 40 μA. The polymer inhibits the growth oxide on the surface of silicon, but does not stop it. Migration of ions either Si^{4+} or OH^{-} through the loosely packed long chain polymer is a likely corrosion mechanism. The nonaqueous couple of ferrocene/ferricenium produced the largest photovoltage, and the polymer was stable to dissolution. However, the experiments indicated that the kinetics of charge transfer through the polymer was very slow, causing a low current level. Capacitance-voltage plots of these systems are similar but difficult to define. An increase in capacitance and pronounced hysteresis coincide with the application of the polymer.

CONCLUSIONS AND RECOMMENDATIONS

The n- and p-type silicon photoelectrochemical cells are capable of producing photovoltages in excess of the antimony redox battery potential, when using the ferrocene and vanadium couples, respectively. However, the stability of the photoelectrode is not sufficient for prolonged operation. In addition, these couples do not meet the critical requirement of both high photovoltage and reasonable solar energy conversion efficiencies. Recent work by Frese [10] illustrates that high efficiency may be obtained at the expense of high stability, and our work substantiates these findings.

Experimental and theoretical investigations have assessed the detrimental effect of the SiO_2 corrosion layer on solar cell characteristics. We found that the oxide thickness must be kept below 15 Å. Treating the surface of silicon with high temperatures under argon or hydrogen, the plating of platinum, and depositing of poly-vinylcarbazole coatings did not significantly suppress the rate of corrosion.

The corrosion of semiconductors in solution is a fundamental problem of photoelectrochemical cells. Silicon, presently, is the most difficult semiconductor to stabilize in solution, compared to binary and layered semiconductors. The corrosion product of silicon, SiO_2, is very stable and quite insoluble in solutions containing ony an inert redox couple. Further research on semiconductors such as Si, or CdSe, or GaAs is needed to increase our understanding of the mechanisms of corrosion and to develop methods to stop the slow degradation of the cell. These suggested studies should focus on the kinetics of the corrosion redox competition. In addition, more work on corrosion suppression using thin metal films and doped polymers would be highly desirable.

Another component of our photobattery is the energy storage system. We believe the antimony redox battery merits further investigation. The antimony redox battery has the advantages of low overvoltage and the 'common ion' product, requiring less stringent anolyte/catholyte compartment separation due to internal short circuit. However, construction of a prototype cell and charge/discharge rates by various electrode materials needs investigating, along with determining effective anolyte and catholyte concentrations for efficient operation of the battery.

REFERENCES

1. S. R. Morrison, in Treatise on Solid State Chemistry, Vol. 6B, N. B. Hannay, ed. (Plenum, New York, 1976), p. 203.
2. J. M. Bolts, A. B. Bocarsly, M. C. Palazzotto, E. G. Walton, N. S. Lewis, and M. S. Wrighton, J. Am. Chem. Soc., 101, 1378 (1979).
3. K. D. Legg, A. B. Ellis, J. M. Bolts, and M. S. Wrighton, Proc. Natl. Acad. Sci.,(USA), 74, 4116 (1977).
4. M. J. Madou, K. W. Frese, and S. R. Morrison, J. Phys. Chem., 84, 3423 (1980).
5. M. J. Madou, K. W. Frese, and S. R. Morrison, SPIE, 2481, (1980).
6. A. B. Bocarsly, E. G. Walton, M. G. Bradley, and M. S. Wrighton, J. Electroanal. Chem., 100, 135 (1981).
7. M. J. Madou, B. H. Loo, K. W. Frese, and S. R. Morrison, Surf. Sci., 108, 135 (1981).
8. W. D. Gill, J. Appl. Phys., 43, 5033 (1972).
9. C. H. Griffiths and A. Van Laeken, J. Polym. Sci., 14, 1433 (1976).
10. K. W. Frese Jr., Appl. Phys. Lett., 40, 275 (1982).

TECHNICAL INFORMATION DEPARTMENT
LAWRENCE BERKELEY LABORATORY
UNIVERSITY OF CALIFORNIA
BERKELEY, CALIFORNIA 94720